Chapter 6

Probing the non-linear structure of general relativity with black hole binaries

6.1 Introduction

Binary pulsar observations provide one of the most stringent methods to test the strong field regime of gravity in general relativity (GR) and its alternatives [212]. The test is possible since the orbital dynamics of the binary is relativistic enough to allow the measurement of effects due to gravitational radiation damping at the post-Newtonian order $(v/c)^5$. Binary pulsar measurements are performed by fitting the pulse arrival times to a relativistic 'timing' model [212, 147, 171, 213] which is a function of the Keplerian parameters (orbital period, eccentricity and the projected semi-major axis of the pulsar orbit) and post-Keplerian (PK) parameters (the periastron advance, time-dilation and secular change of the orbital period). Two more PK parameters, related to the Shapiro-delay caused by the gravitational field of the companion, can be measured if the orbit is seen nearly edge-on. Different theories of gravity have different predictions for the values of the PK parameters as functions of the individual masses of the binary constituents m_1 and m_2. Thus, a measurement of three or more PK parameters facilitates a test by requiring consistency, within the observational errors, in the estimation of the masses of the two bodies as determined by the various parameters. The most rigorous test possible so far is with the most relativistic binary pulsar PSR J0737-3039 [131]. Observed almost edge-on, it permitted the measurement of five PK parameters, which together with an additional constraint from the measurement of mass-ratio, determine and check the consistency of the masses of the two pulsars in the m_1-m_2 plane [131].

As mentioned in the previous chapter, although radio binary pulsars are capable of testing certain lower post-Newtonian (PN) order general relativistic effects, such as the advance of the periastron and the quadrupole approximation to the generation of gravitational waves,

they will, unfortunately, not be able to probe the strong field non-linear effects, such as the tails of gravitational waves [145]. This is because the PN expansion parameter is of order $v \sim 10^{-3}$ – far too small for the effects that first appear at higher post-Newtonian orders to play a significant role in radio observations of binary neutron stars. Space- and ground-based gravitational wave detectors, such as the Laser Interferometer Space Antenna (LISA), Laser Interferometer Gravitational-Wave Observatory (LIGO), VIRGO and European Gravitational-Wave Observatory (EGO), will observe compact binary neutron stars and binary black holes (BBH) in the last stages of their non-linear evolution, during which the parameter v is two orders of magnitude larger (v ~ 0.2-0.4) than it is for current radio observations of such systems. For some of the rare (about once per year) inspiral events observed by LISA (EGO) the amplitude signal-to-noise ratio could be as large as 3,000 (100). Such high SNR events will allow us to measure the parameters of the signal and the source quite accurately, thereby allowing tests that were not feasible earlier. Different tests of GR have been proposed by various authors using GW observations of the inspiralling compact binaries [168, 214, 136, 196] and contrasted with the binary pulsar observations [211]. These tests would necessitate an accurate parameter extraction scheme using the highest PN order waveform available [215].

The GW 'phasing formula' is very close in spirit to the 'timing formula' used in the binary pulsar observations. The timing formula, $\phi_n^{\rm PSR}=F_{\rm T}[t_n, p_i]$, connects the rotational phase ϕ_n of a spinning pulsar to the time-of-arrival t_n of the radio signal and a set of Keplerian and PK parameters $p_i=\{p^K,p^{PK}\}$. Similarly, a precise model for GWs from a compact binary will need accurate information about the continuous evolution of the GW phase. Schematically, the phasing formula reads $\phi^{\rm GW}=F_{\rm P}[t, q_i]$ where, in Einstein's theory, q_i carry the information of the source via functions of the individual masses and spins. The phasing formula consists of different PN parameters q_i, similar to the PK parameters of the timing formula, and is currently available up to relative 3.5PN order *i.e.,* $O(v^7)$ [200, 95, 108, 109, 154].

In the present chapter we propose and explore an interesting possibility of testing General Relativity with the high-SNR GW observations of BBH inspirals by LISA and EGO using a new variant of the proposal discussed in the previous chapter. The proposed test is closer in essence to the binary pulsar test, but in a stronger and dynamic regime of gravity. Given a high SNR binary black hole event one can, in principle, make a model-independent measurement of the various PN coefficients by accepting those values that best fit the data as our estimates. A procedure in which all the parameters $\theta \equiv (t_C, \Phi_C, \psi_k, \psi_{kl})$, k = 0, 2, . . . , 7, are independently varied to obtain the best possible fit of the signal to the data subjects general relativity to the most stringent test possible. In the previous chapter, we explored the power of such a test to determine ***all*** the known coefficients to a relative accuracy of 100% or better [169]. However, this is by no means the most powerful test. This is because the

covariances between the various parameters enhance the errors in their estimation, thereby diluting the effectiveness of the test. In the present chapter we have studied the accuracy with which we can measure the PN coefficients by treating at a time ***only three*** of the nine ψ_k coefficients to be independent and taking the rest as functions of two of the three parameters. Thus, once a high SNR event is identified, we suggest to fit the data to a template wherein ***three*** terms in the PN expansion, rather than just ***two*** as in detection problem, (or ***all*** the PN terms as proposed in Ref. [169]), are treated as independent parameters. Using the two lowest order PN coefficients q_i as basic variables to parametrize the waveform and choosing the other PN coefficients as 'test' parameters, one at a time, it is possible to perform many consistency checks of the PN coefficients in the m_1-m_2 plane. In the rest of the chapter we investigate this possibility in greater detail.

6.2 Testing PN gravity using GW phasing formula

Binary black holes in close orbit around each other are highly relativistic and mandate the inclusion of higher PN order terms in their description. Gravitational waves emitted during the inspiral phase comprise a variety of terms arising from the non-linear multipole interactions as the radiation propagates from the source to the far-zone [63, 158]. These non-linear interactions lead to the phenomenon of tails at orders 1.5PN and 2.5PN (propagation not only on but inside the light cone as well) and tails-of-tails at 3PN. For spinning binaries, there also exist effects of spin-orbit and spin-spin couplings at 1.5PN and 2PN, respectively. These effects are imprinted in the emitted gravitational radiation and can be extracted by matching the detector data with an expected gravitational waveform, often called an optimal filter or a template. The template itself can only be computed using post-Newtonian theory in which the various physical quantities relevant to the emission of gravitational waves are expanded in an asymptotic series in the small parameter v – the characteristic velocity in the system [1]. An important feature of the PN expansion is the presence of log-terms $v^m(\ln v)^n$, where m and n are integers. General relativity is incompatible with a simple Taylor expansion in only powers of v. For instance, currently, the expansions of the specific binding energy E and gravitational wave flux $\mathcal{F}$ are known to order v^7 (i.e. 3.5PN order) and given by

$$E = -\frac{1}{2}\nu v^2 \sum_{k=0}^{3} E_k v^{2k}, \tag{6.1}$$

$$\mathcal{F} = \frac{32}{5}\nu^2 v^{10} \sum_{k=0}^{7} \mathcal{F}_k v^k - \frac{1712}{105}\ln(v) v^6, \tag{6.2}$$

[1]We use a system of units in which $c = G = 1$.

where, $\nu = m_1 m_2 / M^2$, is the symmetric mass ratio in terms of the total mass $M = m_1 + m_2$ and where the coefficients E_k and $\mathcal{F}_k$ can be found in Ref. [26]. Note the presence of the log-term at order v^6 in the expression for the flux.

To understand how we might test the non-linear structure of general relativity let us begin with the Fourier domain representation $H(f)$ of the signal from a binary at a luminosity distance D_L consisting of black holes of masses m_1 and m_2:

$$\tilde{h}(f) = \frac{C\mathcal{M}^{5/6}}{D_L \pi^{2/3}} \sqrt{\frac{5}{24}} f^{-7/6} e^{i\Psi(f) + i\pi/4}, \tag{6.3}$$

where $\mathrm{M} = \nu^{3/5} M$ is the chirp mass and $0 \leq \mathrm{C} \leq 1$ is a constant that depends on the relative orientation of the detector and source with a root-mean-square value of $2/5$ when averaged over all sky locations and source orientations. The phase $\Psi(f)$ is given by

$$\Psi(f) = 2\pi f t_c - \Phi_c + \sum_{k=0}^{7} [\psi_k + \psi_{kl} \ln f] f^{(k-5)/3}. \tag{6.4}$$

Here t_c and Φ_c are the epoch of merger and the signal's phase at that epoch, respectively. ψ_k and ψ_{kl} are independent of f and given by

$$\begin{aligned} \psi_k &= \frac{3}{128\,\nu} (\pi M)^{(k-5)/3} \alpha_k, \\ \psi_{kl} &= \frac{3}{128\,\nu} (\pi M)^{(k-5)/3} \alpha_{kl}, \end{aligned} \tag{6.5}$$

where,

$$\begin{aligned} \alpha_0 &= 1, \quad \alpha_{0l} = 0, \\ \alpha_1 &= 0, \quad \alpha_{1l} = 0, \\ \alpha_2 &= \frac{3715}{756} + \frac{55}{9}\nu, \quad \alpha_{2l} = 0, \\ \alpha_3 &= -16\pi, \quad \alpha_{3l} = 0, \\ \alpha_4 &= \frac{15293365}{508032} + \frac{27145}{504}\nu + \frac{3085}{72}\nu^2, \quad \alpha_{4l} = 0, \\ \alpha_5 &= \pi\left(\frac{38645}{756} - \frac{65}{9}\nu\right)\left[1 + \ln\left(6^{3/2}\pi M\right)\right], \\ \alpha_{5l} &= \pi\left(\frac{38645}{756} - \frac{65}{9}\nu\right), \\ \alpha_6 &= \frac{11583231236531}{4694215680} - \frac{640}{3}\pi^2 - \frac{6848}{21}\gamma \end{aligned}$$

$$
\begin{aligned}
&+ \left(-\frac{15737765635}{3048192} + \frac{2255}{12}\pi^2\right)\nu \\
&+ \frac{76055}{1728}\nu^2 - \frac{127825}{1296}\nu^3 - \frac{6848}{63}\ln(64\pi M), \\
\alpha_{6l} &= -\frac{6848}{63}, \\
\alpha_7 &= \pi\left(\frac{77096675}{254016} + \frac{378515}{1512}\nu - \frac{74045}{756}\nu^2\right), \\
\alpha_{7l} &= 0.
\end{aligned} \tag{6.6}
$$

The non-vanishing coefficients of the log-terms up to 3.5PN are

$$\psi_{5l} = -\frac{65\pi}{384} + \frac{38645\pi}{32256\nu} \tag{6.7a}$$

and

$$\psi_{6l} = -\frac{107}{42\nu}(\pi M)^{1/3}. \tag{6.7b}$$

We have a total of nine post-Newtonian parameters, seven of these are the coefficients of v^n terms for n = 0, 2, 3, 4, 5, 6, 7, and two are coefficients of $v^n \ln(v)$ terms for n = 5, 6,[2] but each of these parameters depends only on the masses of the two black holes for the nonspinning case in GR.

As in the previous chapter, we assume a cosmological model with zero spatial curvature $\Omega_\kappa = 0$, matter density $\Omega_\Lambda + \Omega_M = 1$ and Hubble's constant $H_0 = 70$ km s^{-1} Mpc^{-1}. The luminosity distance as mentioned earlier

$$D_L = \frac{c(1+z)}{H_0}\int_0^z \frac{dz'}{[\Omega_M(1+z')^3 + \Omega_\Lambda]^{1/2}}, \tag{6.8}$$

where z denotes the redshift of the source.

6.3 Model of the gravitational waveform and assumptions involved

Before proceeding with the description of our work, let us summarise the assumptions implicit in the analysis, the justification for doing so and their possible implications. As in most works on this subject, to demonstrate the 'principle' of the proposed method we neglect the effects of spins and eccentricity. What will change on including these additional parameters is the accuracy of the test. The spin effects are relevant only when one of the black holes is

[2] In the Fourier domain the log-terms appear at 2.5PN order rather than 3PN because of an integration that involves 1/f.

much smaller than the other and/or when the black holes have their dimensionless spin angular momentum close to unity. It is not clear that astrophysical black holes, especially the supermassive ones, will be extreme Kerr. Except in cases where both BHs are extreme Kerr (or close to it) spin effects are less important for the proposed tests since we have considered black holes of comparable masses in our study. The issue of eccentricity, especially for certain LISA sources, is a complex issue depending on the astrophysical scenario related to formation mechanisms of the binary. Our neglect of eccentricity is a simplifying assumption at present. Finally, let us comment on the use of the so-called restricted PN waveform in this work. Not merely in connection with tests that have been proposed but more seriously in most works related to the detection problem in GW data analysis, the late inspiral and merger part is ignored in the first instance. One begins by using state-of-the-art restricted PN inspiral templates. This is not just a theoretical convenience but appropriate as well since both for EGO and for LISA there would be a sub-class of sources that would be inspiral-dominated. By the time LISA and EGO operate there could be reliable merger waveforms that can be included in the phasing and this would make this test more robust.

6.4 Implementation of the proposed test

As mentioned earlier, given a high SNR binary black hole event one can, in principle, make a model-independent measurement of the various above PN coefficients by accepting those values that best fit the data as our estimates. We now investigate the accuracy with which one can measure the PN coefficients by treating at a time just three of the nine ψ_k coefficients to be independent and taking the rest as functions of two of the three parameters. More precisely, in Einstein's GR, the tests consist in treating the parameters ψ_0 and ψ_2 as the fundamental ones from which we can measure the masses of the two black holes by inverting the relationships $\psi_0 = \psi_0(m_1, m_2)$ and $\psi_2 = \psi_2(m_1, m_2)$, and asking if the measurement of a third parameter, say $\psi_{6l} = \psi_{6l}(m_1, m_2)$, is consistent with the other two. Instead of the pair (ψ_0, ψ_2) one can, in principle, equally well take any other pair to be the fundamental set. The parameters ψ_0 and ψ_2, being lower order coefficients, are best determined as compared to the others and constitute our favoured pair. In analogy with the binary pulsar case each PN order coefficient can be thought of as comprising different physical effects. The determination of a particular PN coefficient is thus the measurement of particular PN effects. The possibility to confirm the PN coefficients is what we principally explore and for that what we propose is appropriate. The proposal to check a fundamental feature about PN theory such as the presence of log-terms by measuring the relevant parameter directly from observations is significant. One could alternatively use the entire PN expansion up to some order k' as a basis, and then check consistency with $\psi_{k'+1}$ (ignoring higher order terms). This would

be relevant for testing alternative theories where deviations from GR may grow larger with stronger gravity. The procedure we prescribe has the advantage over the above scheme that even if one is testing a low order PN coefficient, the systematic effects arising from neglect of higher PN order terms is controlled to the extent possible.

We shall consider the estimation of parameters using the covariance matrix, in the ground-based EGO and space-based LISA cases, for which we assume the noise PSDs as given in Ref. [216] and [208], respectively. We shall take the fundamental parameters to be ψ_0 and ψ_2 in addition to the usual extrinsic parameters t, and Φ_c. We shall take the test parameter ψ_T to be in turn $\psi_3, \ldots, \psi_7$, ψ_{5l} and ψ_{6l}. It should be noted that as in the previous chapter there is no test corresponding to the term involving ψ_5 since it has no frequency dependence and simply leads to a shift in the coalescence phase Φ_c.

For ground-based detectors, Advanced LIGO and EGO, each (independent) test involves the parameters t_c, Φ_c and the three chosen ψ_k's. For LISA, on the other hand, the results correspond to the case of a single detector but with amplitude modulation caused by the motion of the detector relative to the source. Thus, for LISA our Fourier domain waveform will have amplitude, phase and frequency modulations due to the orbital motion of LISA and we use the waveform given in Ref [207]. In the case of LISA, in addition to the three ψ_k parameters related to our tests we also have the luminosity distance D_L and the four angles related to the source's location and orientation $\mu_S = \cos\bar{\theta}_S$, $\bar{\phi}_S$, $\mu_L = \cos\bar{\theta}_L$, $\bar{\phi}_L$.

6.4.1 SNR for Advanced LIGO, EGO and LISA

The power of the tests depends on the SNR achieved for the source. In Fig. [6.1] we have plotted the SNR in LISA, EGO and for comparison, Advanced LIGO [215], for BBH binaries at a distance of $z = 1$ for LISA and a distance of $D_L = 200$ Mpc for EGO and Advanced LIGO. In the case of EGO, we consider stellar mass BBH of equal masses with the total mass in the range $1M_\odot$ to $400M_\odot$, while in the case of LISA the mass range is from $10^4 M_\odot$ to $10^7 M_\odot$, but scaled down by 10^4 so as to fit all the curves in the same plot. While the SNR in EGO can reach several 100's for sources that it might observe every once in a year, in the case of LISA the SNR could be several 1,000's for the supermassive BBH sources that it is expected to observe about once per year. The SNR's in both LISA and EGO are large enough for the tests to be powerful probes of the PN coefficients and the non-linear effects of GR.

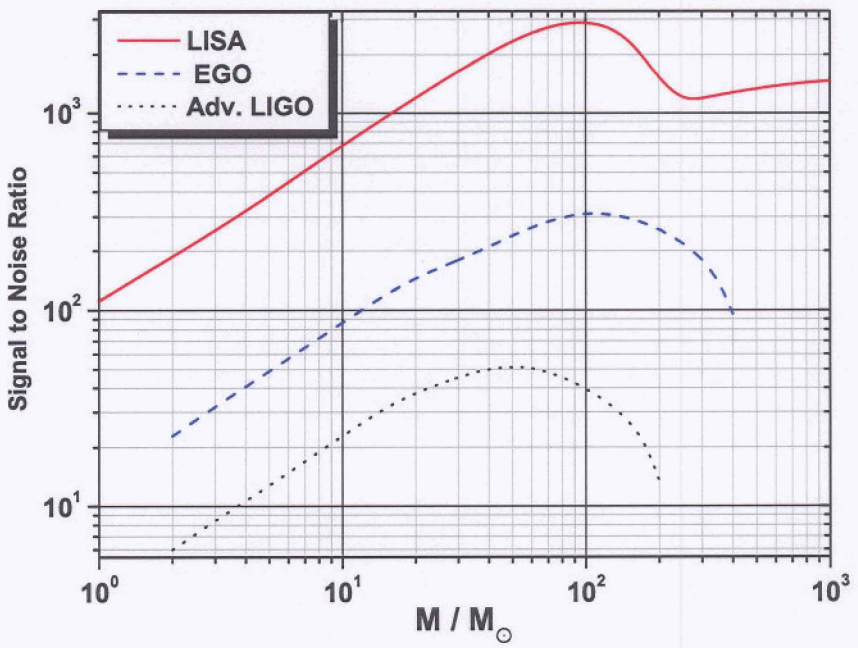

Figure 6.1: The signal-to-noise ratio for stellar mass binary black holes (BBH) in Advanced LIGO and EGO and **supermassive BBH** in **LISA** for **equal mass binaries at a distance** of **200 Mpc (for EGO and Advanced LIGO) and** $z = 1$ **(LISA) respectively. In the case** of **LISA we assume that the signal is integrated** for **a year (last year** before **coalescence) and in the case** of EGO **we assume that the signal** is **integrated over a bandwidth from 10 Hz** until **the binary** reaches **its** innermost circular **orbit. The masses of** supermassive **BBH** in **the case of LISA have** been **scaled down** by **a factor of** 10^4. The maximum **SNR for** Advanced **LIGO, EGO and LISA is 52, 310, 2922 respectively corresponding to the** total **binary mass** of $55M_\odot$, $112M_\odot$, $10^6 M_\odot$.

6.4.2 The test using Advanced LIGO

Let us begin with the case of Advanced LIGO. For a source at 200 Mpc the errors in the lowest order parameters ψ_0 and ψ_2 are measured with the smallest relative errors of order $10^{-4} - 10^{-2}$. Fig. [6.2] plots the relative errors $\Delta\psi_T/\psi_T$ for various parameters ψ_T as a function of the total mass M. From the plots, it is clear that the proposed tests can be performed only for ψ_3 and ψ_{5l} with fractional accuracies better than 100% for stellar mass BBH binaries with the total mass in the range 2-50 $M_\odot$. For sources with the total mass in a very narrow range around $\sim 15M_\odot$, all the parameters, except ψ_4 and ψ_{6l}, can also be measured to a relative accuracy of 100%. Thus, though the 3PN log-term cannot be probed with Advanced LIGO, the 2.5PN log-term can be tested leading to an interesting possibility in the more immediate future.

6.4.3 The test using EGO

In the case of EGO for a source at 200 Mpc the errors in the lowest order parameters ψ_0 and ψ_2 are measured with the smallest errors of order $10^{-5} - 10^{-3}$. Fig. [6.3] plots the relative errors $\Delta\psi_T/\psi_T$ for various parameters ψ_T as a function of the total mass M. From the plots, it is clear that the proposed tests can be performed for ***all*** ψ_k's, with fractional accuracies better than 100% for stellar mass BBH binaries with the total mass in the range $5\text{-}14M_\odot$. This demonstrates the exciting possibility of testing the non-linear structure of general relativity using the GW observations by EGO. More quantitative details including the relevant correlation coefficients are summarized in Tables [6.1] - [6.6].
From those tables [6.1] -[6.6] and fig. [6.4] of the correlations for EGO, we find the following:

- The correlation coefficients in general are very much mass dependent.
- The correlation coefficient c^{24} is almost constant (varying between 0.9997-1) for binary total masses in the range $2 - 200M_\odot$. Thus variables ψ_2 and ψ_4 are very strongly correlated.

  The correlation coefficient c^{02}, for test variables ψ_T (T = 51, 6, 61, 7) increases from 0.84 to 1.0 when the binary mass varies from $2M_\odot$ to $200M_\odot$. Thus variables ψ_0 and ψ_2 are also correlated. However the correlation varies from strong to very strong depending on the binary mass.
- The correlation coefficient c^{0T} (T = 51, 6, 61, 7) similarly increases from –1 to –.75 as the total mass varies from $2M_\odot$ to $200M_\odot$. Thus the parameter ψ_0 and ψ_T, (T =

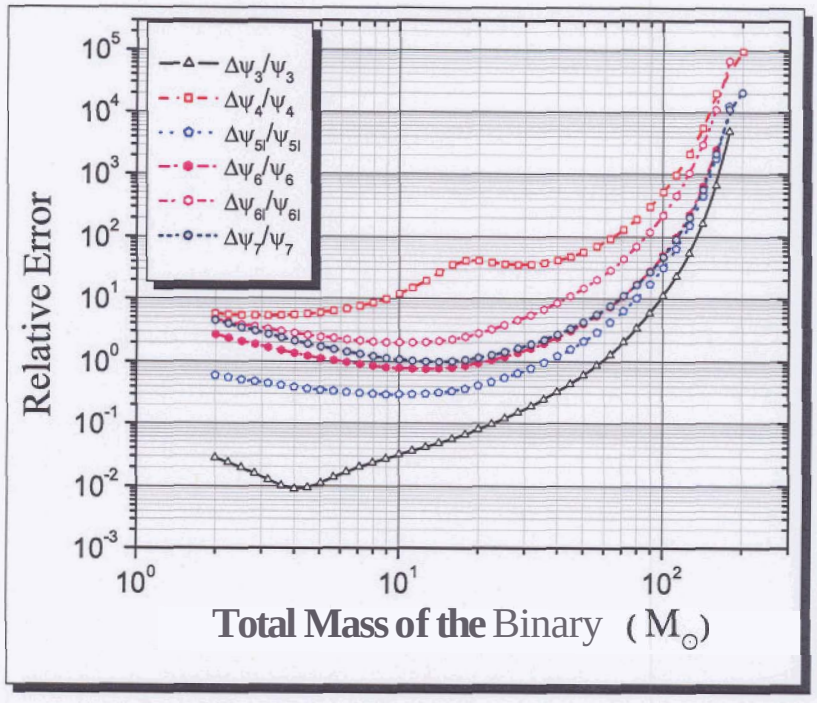

Figure *6.2:* **Plot showing the relative errors** $\Delta\psi_T/\psi_T$, **in the** test **parameters** $\psi_T = \psi_3, \psi_4, \psi_{5l}, \psi_6, \psi_{6l}, \psi_7$, **as a function of the** total **mass** M **of a BBH at a distance** of $D_L = 200$ Mpc observed **by Advanced LIGO. We assume that the signal** is **integrated over a bandwidth from 20 Hz** until the binary **reaches its innermost** circular orbit. **The proposed tests** can be **performed only** for ψ_3 **and** ψ_{5l} **(with fractional accuracies better** than **100%)** *for* **stellar mass BBH binaries with** total **mass in the range** 2-50 $M_\odot$. **For sources with the total mass in a very** narrow range **around** $\sim 15M_\odot$, *all* **the parameters,** *except* ψ_4 and ψ_{6l}, can **be** similarly **measured.**

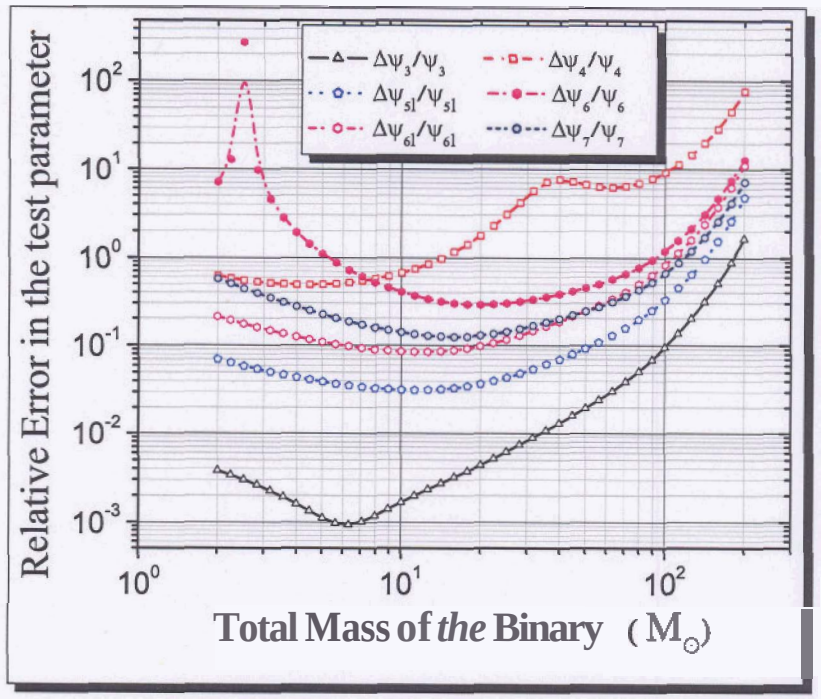

Figure 6.3: Plot showing **the** relative errors $\Delta\psi_T/\psi_T$, in **the test parameters** $\psi_T = \psi_3, \psi_4, \psi_{5l}, \psi_6, \psi_{6l}, \psi_7$, **as a** function of **the total mass** M ***of*** **a BBH at a distance of** $D_L =$ 200 Mpc observed by EGO. **We assume that the signal is integrated over a** bandwidth from 10 Hz until **the binary reaches** its innermost **circular** orbit. The **proposed tests can be performed** for *all* ψ_k's, **with fractional accuracies** better **than** 100% for stellar **mass** BBH binaries **with** total **mass** in **the range** 5-14$M_\odot$.

51, 6, 61, 7) are always anti-correlated.

- The correlation coefficient c^{02} (when $\psi_T = \psi_3$) varies between -0.98 and -0.95 in the same mass range. Thus parameters ψ_0 and ψ_3 are strongly anti-correlated.

- The correlation coefficient c^{02} (when $\psi_T = \psi_4$) and c^{24} vary over the full range $[-1, 1]$ as the total mass varies between $2 - 200 M_\odot$. They are positive in the mass range between 3 and 100 solar mass and negative in the rest of the range.

- The correlation coefficients c^{03} and c^{23} vary in the full range $[-1, 1]$ very similarly, but relatively differ by a sign. $c^{03}(c^{23})$ starts from $+1(-1)$ decreases through zero at a mass of about $5.5 M_\odot$ and then saturates at $-1(+1)$ from a total mass value of $10 M_\odot$ up to $200 M_\odot$.

6.4.4 The test using LISA

In the case of LISA the errors in the parameters ψ_0 and ψ_2 for a source at $z = 1$ are of order $10^{-7} - 10^{-6}$ in the range of the total mass 10^4-10^7 $M_\odot$. The cosmological model used is ($\Omega_\kappa = 0, \Omega_M = 0.3$ and $\Omega_\Lambda = 0.7$) and the redshift is $z = 1$. Fig. [6.5] plots the relative errors $\Delta\psi_T/\psi_T$ for various parameters ψ_T as a function of the total mass M. The top panel corresponds to the relative errors when the waveform model includes the orientation of the source. The orientation of the source is chosen to be $(\cos\bar{\theta}_S, \bar{\phi}_S, \cos\bar{\theta}_L, \bar{\phi}_L) = (09, 2, -0.8, -5)$. The bottom panel corresponds to the averaged pattern waveform. From the plots, it is clear that the proposed tests can be performed effectively with ***all*** ψ_k***'s. This is another reason why LISA is such an important mission.*** All the test parameters, including the log-terms at 2.5PN and 3PN order, can be estimated with fractional accuracies better than 10^{-2} for massive BBH binaries with the total mass in the range 10^4-10^7 $M_\odot$[3]. This demonstrates the exciting possibility of testing the non-linear structure of general relativity using the GW observations of LISA. Further quantitative details like the correlation coefficients are tabulated in Tables 6.7 - 6.12 for LISA with the pattern averaged waveform. The more complex case without pattern averaging *i.e.* with a specific choice of 'optimal' orientation angles is also investigated. The details are summarised in Tables 6.13 - 6.18.

6.4.5 No test for ψ_4 ?

With reference to Fig. [6.3] and [6.5], one may wonder why the error in ψ_4 is the largest relative to the other higher order ψ_k's. We believe that there are several reasons for this odd

[3]It should be emphesized that here one is only talking about the statistical errors and that the systematic errors (i.e. biases) might dominate over the statistical errors and must be investigated in the future

Table 6.1: Variation with total binary mass M of SNR, the relative errors in the ψ_0, ψ_2 and ψ_3 for EGO when the test parameter is ψ_3. The luminosity distance is $D_L = 200$ Mpc. Also listed are the correlation coefficients $c^{ij} = c^{ji}$ between the parameters ψ_i and ψ_j, $i, j = 0, 2, 3$.

$M\,(M_\odot)$	SNR	$\Delta\psi_0/\psi_0\%$	$\Delta\psi_2/\psi_2\%$	$\Delta\psi_3/\psi_3\%$	c^{02}	c^{03}	c^{23}
2	22.8	0.00708	0.431	0.380	-0.970	0.882	-0.968
$2\times10^{0.25}$	36.8	0.0107	0.383	0.192	-0.963	0.726	-0.878
$2\times10^{0.5}$	59.4	0.0170	0.343	0.0934	-0.957	-0.303	0.0320
$2\times10^{0.75}$	94.9	0.0299	0.331	0.199	-0.953	-0.961	0.848
$2\times10^{1.}$	144.	0.0630	0.392	0.440	-0.955	-0.997	0.946
$2\times10^{1.25}$	196.	0.172	0.618	1.08	-0.963	-0.998	0.973
$2\times10^{1.5}$	270.	0.577	1.12	3.08	-0.969	-0.998	0.982
$2\times10^{1.75}$	310.	3.07	2.99	13.6	-0.975	-0.999	0.986
$2\times10^{2.}$	257.	45.4	18.4	165.	-0.980	-0.999	0.986

Table 6.2: A similar table as above for the test parameter ψ_4. Also listed are the correlation coefficients c^{ij} between the parameters ψ_i and ψ_j, $i, j = 0, 2, 4$.

$M\,(M_\odot)$	SNR	$\Delta\psi_0/\psi_0\%$	$\Delta\psi_2/\psi_2\%$	$\Delta\psi_4/\psi_4\%$	c^{02}	c^{04}	c^{24}
2	22.8	0.00302	1.33	62.2	-0.906	-0.915	1.00
$2\times10^{0.25}$	36.8	0.00221	1.11	50.0	0.293	0.272	1.00
$2\times10^{0.5}$	59.4	0.00752	1.21	52.2	0.878	0.869	1.00
$2\times10^{0.75}$	94.9	0.0232	1.79	74.9	0.961	0.957	1.00
$2\times10^{1.}$	144.	0.0878	4.35	178.	0.989	0.988	1.00
$2\times10^{1.25}$	196.	0.452	17.7	714.	0.998	0.998	1.00
$2\times10^{1.5}$	270.	0.367	15.3	619.	0.975	0.974	1.00
$2\times10^{1.75}$	310.	0.331	27.4	1140	0.244	0.232	1.00
$2\times10^{2.}$	257.	9.92	177.	7720	-0.956	-0.960	1.00

Table *6.3:* Variation with total binary mass M of SNR, the relative errors in the ψ_0, ψ_2 and ψ_{5l} for EGO when the test parameter is ψ_{5l}. The luminosity distance is $D_L = 200$ Mpc. Also listed are the correlation coefficients $c^{ij} = c^{ji}$ between the parameters ψ_i and ψ_j, $i, \mathrm{j} = 0, 2, 5\mathrm{l}$.

$M\,(M_\odot)$	SNR	$\Delta\psi_0/\psi_0\%$	$\Delta\psi_2/\psi_2\%$	$\Delta\psi_{5l}/\psi_{5l}\%$	c^{02}	c^{05l}	c^{25l}
2	22.8	0.00193	0.254	6.94	0.843	-0.760	-0.986
$2\times10^{0.25}$	36.8	0.00422	0.226	4.68	0.914	-0.845	-0.986
$2\times10^{0.5}$	59.4	0.00869	0.226	3.54	0.943	-0.885	-0.987
$2\times10^{0.75}$	94.9	0.0184	0.262	3.16	0.961	-0.912	-0.988
$2\times10^{1.}$	144.	0.0441	0.388	3.70	0.975	-0.938	-0.991
$2\times10^{1.25}$	196.	0.133	0.793	6.15	0.986	-0.962	-0.994
$2\times10^{1.5}$	270.	0.486	2.05	12.8	0.993	-0.979	-0.996
$2\times10^{1.75}$	310.	2.83	8.88	45.0	0.997	-0.991	-0.998
$2\times10^{2.}$	257.	45.7	113.	473.	0.999	-0.997	-0.999

Table *6.4:* A similar table as above for the test parameter ψ_6. Also listed are the correlation coefficients c^{ij} between the parameters ψ_i and ψ_j, i, $\mathrm{j} = 0, 2, 6$.

$M\,(M_\odot)$	SNR	$\Delta\psi_0/\psi_0\%$	$\Delta\psi_2/\psi_2\%$	$\Delta\psi_6/\psi_6\%$	c^{02}	c^{06}	c^{26}
2	22.8	0.00192	0.140	710.	0.885	-0.769	-0.967
$2\times10^{0.25}$	36.8	0.00384	0.127	279.	0.924	-0.826	-0.970
$2\times10^{0.5}$	59.4	0.00757	0.127	72.5	0.945	-0.864	-0.974
$2\times10^{0.75}$	94.9	0.0155	0.146	36.6	0.961	-0.894	-0.979
$2\times10^{1.}$	144.	0.0361	0.211	28.9	0.974	-0.923	-0.984
$2\times10^{1.25}$	196.	0.106	0.422	35.6	0.986	-0.953	-0.990
$2\times10^{1.5}$	270.	0.374	1.06	56.7	0.993	-0.973	-0.993
$2\times10^{1.75}$	310.	2.09	4.43	157.	0.997	-0.987	-0.996
$2\times10^{2.}$	257.	32.1	53.7	1300	0.999	-0.996	-0.999

Table 6.5: Variation with total binary mass M of SNR, the relative errors in the ψ_0, ψ_2 and ψ_{6l} for EGO when the test parameter is ψ_{6l}. The luminosity distance is D_L = 200 Mpc. Also listed are the correlation coefficients $c^{ij} = c^{ji}$ between the parameters ψ_i and ψ_j, i, j = 0, 2, 6l.

$M\,(M_\odot)$	SNR	$\Delta\psi_0/\psi_0\%$	$\Delta\psi_2/\psi_2\%$	$\Delta\psi_{6l}/\psi_{6l}\%$	c^{02}	c^{06l}	c^{26l}
2	22.8	0.00188	0.117	21.1	0.892	-0.768	-0.959
$2\times10^{0.25}$	36.8	0.00369	0.106	13.5	0.926	-0.824	-0.965
$2\times10^{0.5}$	59.4	0.00719	0.106	9.81	0.947	-0.863	-0.972
$2\times10^{0.75}$	94.9	0.0146	0.122	8.51	0.962	-0.895	-0.978
$2\times10^{1.}$	144.	0.0337	0.174	9.84	0.975	-0.924	-0.984
$2\times10^{1.25}$	196.	0.0974	0.344	16.4	0.986	-0.952	-0.989
$2\times10^{1.5}$	270.	0.342	0.852	33.4	0.993	-0.972	-0.993
$2\times10^{1.75}$	310.	1.88	3.51	113.	0.997	-0.987	-0.996
$2\times10^{2.}$	257.	28.5	42.0	1120	0.999	-0.996	-0.998

Table 6.6: **A** similar table as above for the test parameter ψ_7. Also listed are the correlation coefficients c^{ij} between the parameters ψ_i and ψ_j, i, j = 0, 2, 7.

$M\,(M_\odot)$	SNR	$\Delta\psi_0/\psi_0\%$	$\Delta\psi_2/\psi_2\%$	$\Delta\psi_7/\psi_7\%$	c^{02}	c^{07}	c^{27}
2	22.8	0.00178	0.0966	57.5	0.892	-0.726	-0.933
$2\times10^{0.25}$	36.8	0.00346	0.0889	30.7	0.924	-0.783	-0.942
$2\times10^{0.5}$	59.4	0.00671	0.0899	18.5	0.945	-0.826	-0.951
$2\times10^{0.75}$	94.9	0.0136	0.103	13.3	0.960	-0.861	-0.959
$2\times10^{1.}$	144.	0.0312	0.149	12.9	0.974	-0.896	-0.969
$2\times10^{1.25}$	196.	0.0899	0.296	18.2	0.986	-0.933	-0.978
$2\times10^{1.5}$	270.	0.314	0.739	31.0	0.993	-0.960	-0.986
$2\times10^{1.75}$	310.	1.73	3.08	87.4	0.997	-0.980	-0.992
$2\times10^{2.}$	257.	26.2	37.3	715.	0.999	-0.993	-0.997

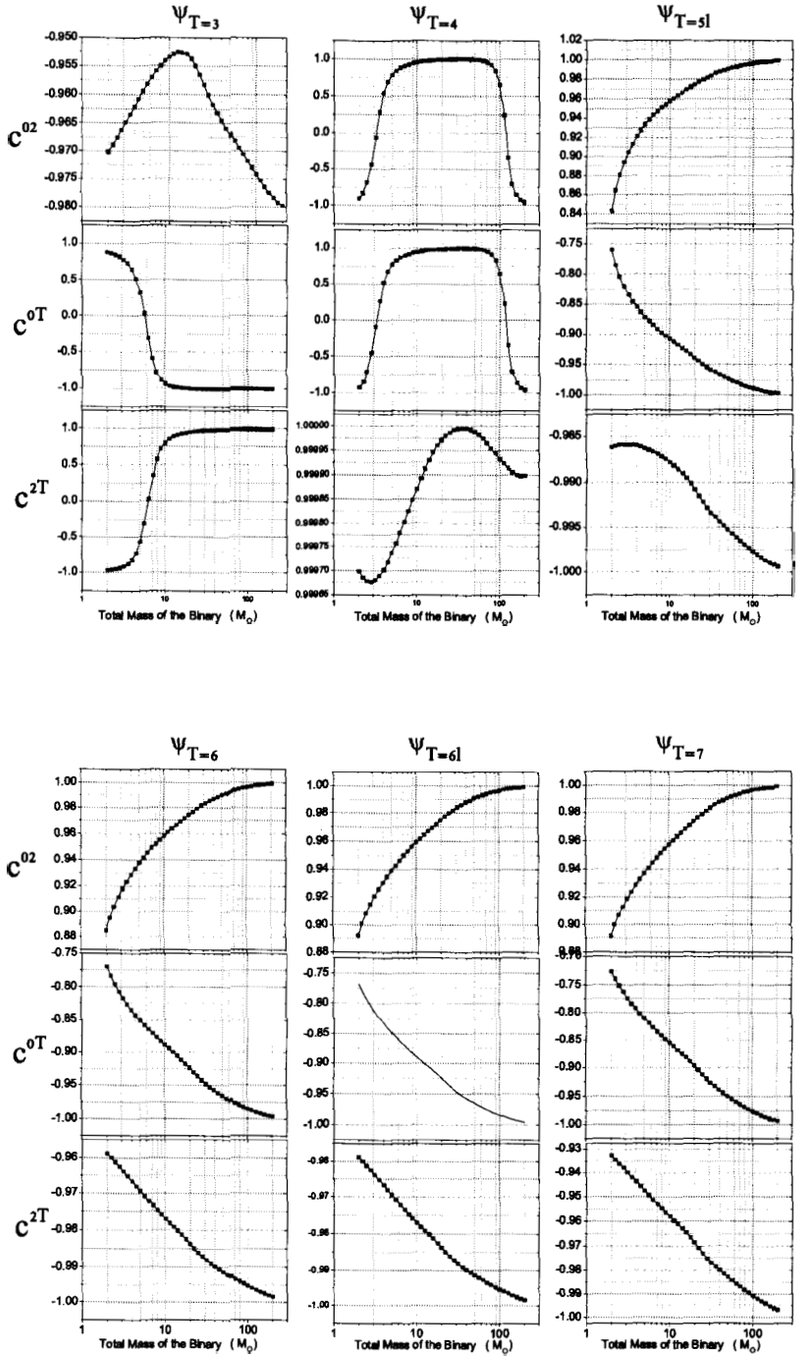

Figure 6.4: Plot showing the variation of the correlation coefficients c^{iT} for EGO with the total mass of the binary. The luminosity distance is D_L = 200 Mpc. c^{iT} is the correlation coefficient between ψ_i, i = 0, 2 and the test parameter ψ_T, T = 3, 4, 5l, 6, 6l, 7.

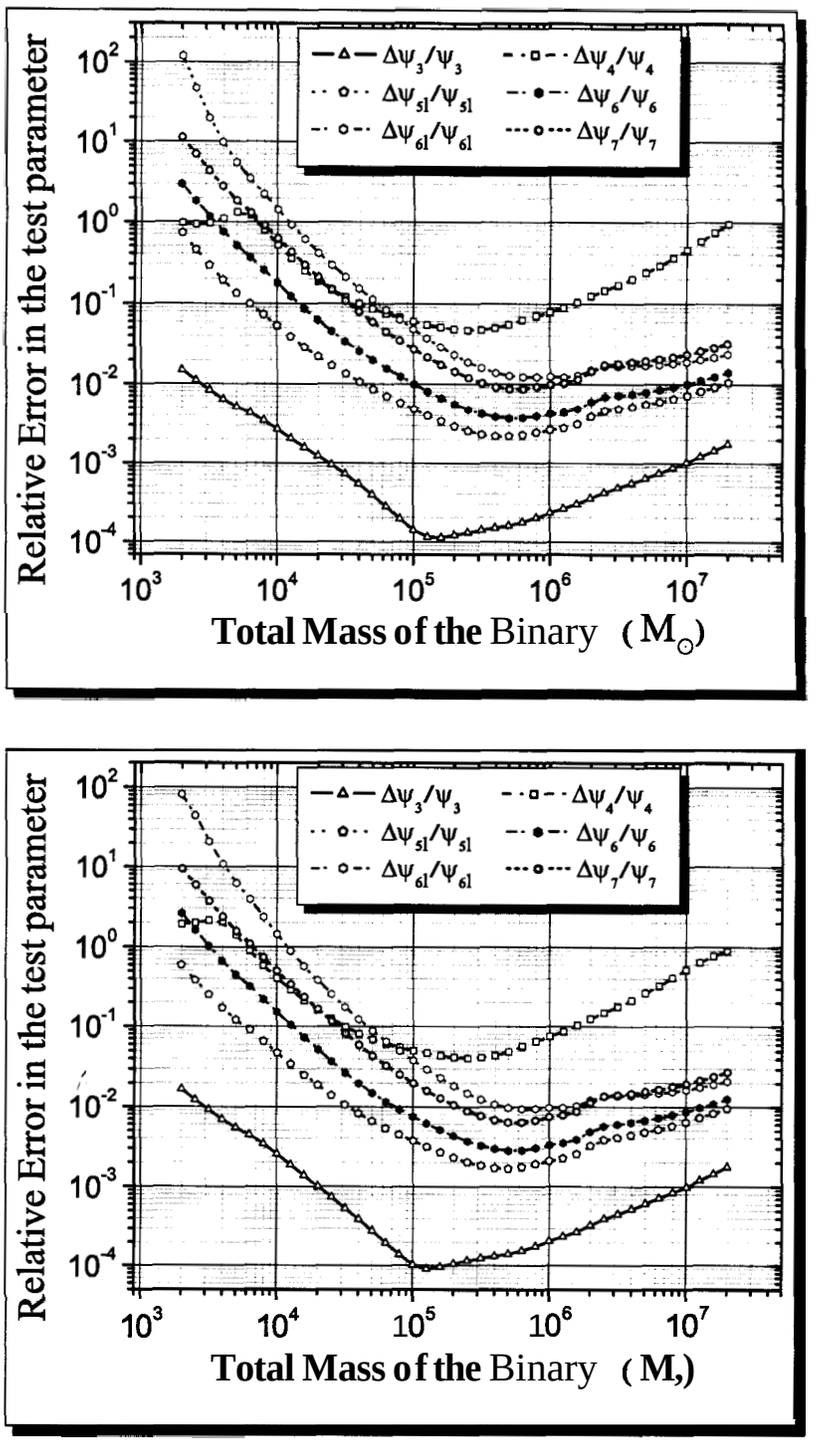

Figure 6.5: Plot showing the relative errors $\Delta\psi_T/\psi_T$, in the test parameters $\psi_T = \psi_3, \psi_4, \psi_{51}, \psi_6, \psi_{61}, \psi_7$, as a function of the total mass M of a supermassive BBH at a redshift of $z = 1$ observed by LISA. We assume that the signal is integrated for a year. The cosmological model used is (R, = 0, $\Omega_M = 0.3$ and $\Omega_\Lambda = 0.7$). The top figure corresponds to a waveform including a particular 'optimum' orientation of the source $(\cos\bar{\theta}_S, \bar{\phi}_S, \cos\bar{\theta}_L, \bar{\phi}_L)$ = (0.9, 2, –0.8, –5). The bottom figure corresponds to the averaged pattern waveform. In both cases all the ψ_k's can be tested in the total binary mass range 10^4-2 x $10^6 M_\odot$.

Table 6.7: Variation with total binary mass M of SNR, the relative errors in the ψ_0, ψ_2 and ψ_3 for LISA when the test parameter is ψ_3. The cosmological model used is ($\Omega_\kappa = 0$, $\Omega_M = 0.3$ and $\Omega_\Lambda = 0.7$) and the redshift is $z = 1$. The waveform model corresponds to the pattern averaged case. Also listed are the correlation coefficients $c^{ij} = c^{ji}$ between the parameters ψ_i and ψ_j, $i, j = 0, 2, 3$.

$M\,(M_\odot)$	SNR$\times 10^3$	$\Delta\psi_0/\psi_0\%$	$\Delta\psi_2/\psi_2\%$	$\Delta\psi_3/\psi_3\%$	c^{02}	c^{03}	c^{23}
$2\times10^{3.}$	0.0148	0.00302	0.685	1.49	−0.991	0.976	−0.996
$2\times10^{3.5}$	0.0437	0.00206	0.270	0.429	−0.985	0.959	−0.993
$2\times10^{4.}$	0.115	0.00160	0.117	0.123	−0.967	0.903	−0.981
$2\times10^{4.5}$	0.299	0.00143	0.0558	0.0278	−0.960	0.721	−0.872
$2\times10^{5.}$	0.776	0.00141	0.0276	0.0121	−0.934	−0.698	0.452
$2\times10^{5.5}$	1.71	0.00193	0.0236	0.0176	−0.909	−0.945	0.784
$2\times10^{6.}$	0.972	0.00436	0.0406	0.0354	−0.930	−0.981	0.886
$2\times10^{6.5}$	0.896	0.00987	0.0624	0.0745	−0.936	−0.993	0.936
$2\times10^{7.}$	0.935	0.0253	0.106	0.175	−0.942	−0.995	0.959

Table **6.8:** A similar table as above for the test parameter ψ_4. Also listed are the correlation coefficients c^{ij} between the parameters ψ_i and ψ_j, i, j = 0, 2, 4.

$M\,(M_\odot)$	SNR$\times 10^3$	$\Delta\psi_0/\psi_0\%$	$\Delta\psi_2/\psi_2\%$	$\Delta\psi_4/\psi_4\%$	c^{02}	c^{04}	c^{24}
$2\times10^{3.}$	0.0148	0.00618	2.10	97.5	−0.999	−1.00	0.999
$2\times10^{3.5}$	0.0437	0.00829	2.48	122.	−1.00	−1.00	1.00
$2\times10^{4.}$	0.115	0.00106	0.390	18.6	−0.955	−0.960	1.00
$2\times10^{4.5}$	0.299	0.000310	0.168	7.54	−0.0284	−0.0471	1.00
$2\times10^{5.}$	0.776	0.000649	0.113	4.82	0.816	0.805	1.00
$2\times10^{5.5}$	1.71	0.00143	0.150	6.28	0.909	0.903	1.00
$2\times10^{6.}$	0.972	0.00396	0.297	12.3	0.956	0.952	1.00
$2\times10^{6.5}$	0.896	0.0128	0.703	28.8	0.981	0.980	1.00
$2\times10^{7.}$	0.935	0.0524	2.36	96.0	0.994	0.993	1.00

Table 6.9: Variation with total binary mass M of SNR, the relative errors in the ψ_0, ψ_2 and ψ_{5l} for LISA when the test parameter is ψ_{5l}. The cosmological model used is ($\Omega_\kappa = 0$, $\Omega_M = 0.3$ and $\Omega_\Lambda = 0.7$) and the redshift is $z = 1$. The waveform model corresponds to the pattern averaged case. Also listed are the correlation coefficients $c^{ij} = c^{ji}$ between the parameters ψ_i and ψ_j, i, j = 0, 2, 5l.

$M\,(M_\odot)$	SNR$\times 10^3$	$\Delta\psi_0/\psi_0\%$	$\Delta\psi_2/\psi_2\%$	$\Delta\psi_{5l}/\psi_{5l}\%$	c^{02}	c^{05l}	c^{25l}
$2\times10^{3.}$	0.0148	0.00265	1.29	72.4	−0.997	0.999	−0.997
$2\times10^{3.5}$	0.0437	0.000254	0.219	9.79	−0.609	0.693	−0.992
$2\times10^{4.}$	0.115	0.000391	0.0693	2.17	0.734	−0.637	−0.987
$2\times10^{4.5}$	0.299	0.000545	0.0339	0.694	0.872	−0.806	−0.986
$2\times10^{5.}$	0.776	0.000773	0.0210	0.288	0.913	−0.842	−0.980
$2\times10^{5.5}$	1.71	0.00121	0.0201	0.226	0.914	−0.832	−0.979
$2\times10^{6.}$	0.972	0.00288	0.0366	0.387	0.944	−0.885	−0.986
$2\times10^{6.5}$	0.896	0.00701	0.0641	0.595	0.960	−0.913	−0.989
$2\times10^{7.}$	0.935	0.0193	0.130	1.04	0.973	−0.936	−0.991

Table 6.10: **A** similar table as above for the test parameter ψ_6. Also listed are the correlation coefficients c^{ij} between the parameters ψ_i and ψ_j, i, j = 0, 2, 6.

$M\,(M_\odot)$	SNR$\times 10^3$	$\Delta\psi_0/\psi_0\%$	$\Delta\psi_2/\psi_2\%$	$\Delta\psi_6/\psi_6\%$	c^{02}	c^{06}	c^{26}
$2\times10^{3.}$	0.0148	0.000700	0.476	301.	−0.968	0.991	−0.985
$2\times10^{3.5}$	0.0437	0.000207	0.106	35.8	0.606	−0.441	−0.975
$2\times10^{4.}$	0.115	0.000410	0.0372	6.18	0.822	−0.694	−0.969
$2\times10^{4.5}$	0.299	0.000503	0.0189	1.55	0.875	−0.791	−0.976
$2\times10^{5.}$	0.776	0.000694	0.0124	0.555	0.911	−0.838	−0.976
$2\times10^{5.5}$	1.71	0.00106	0.0113	0.373	0.911	−0.825	−0.976
$2\times10^{6.}$	0.972	0.00246	0.0205	0.596	0.941	−0.880	−0.984
$2\times10^{6.5}$	0.896	0.00587	0.0354	0.853	0.958	−0.909	−0.988
$2\times10^{7.}$	0.935	0.0158	0.0709	1.40	0.971	−0.933	−0.991

Table 6.11: Variation with total binary mass M of SNR, the relative errors in the ψ_0, ψ_2 and ψ_{6l} for LISA when the test parameter is ψ_{6l}. The cosmological model used is ($\Omega_\kappa = 0$, $\Omega_M = 0.3$ and $\Omega_\Lambda = 0.7$) and the redshift is $z = 1$. The waveform model corresponds to the pattern averaged case. Also listed are the correlation coefficients $c^{ij} = c^{ji}$ between the parameters ψ_i and ψ_j, i, $j = 0, 2, 6l$.

$M\,(M_\odot)$	SNR$\times 10^3$	$\Delta\psi_0/\psi_0\%$	$\Delta\psi_2/\psi_2\%$	$\Delta\psi_{6l}/\psi_{6l}\%$	c^{02}	c^{06l}	c^{26l}
$2\times10^{3.}$	0.0148	0.0127	5.85	11900	−1.00	−1.00	1.00
$2\times10^{3.5}$	0.0437	0.000323	0.321	351.	−0.779	−0.819	0.997
$2\times10^{4.}$	0.115	0.000436	0.0773	41.4	0.798	0.733	0.993
$2\times10^{4.5}$	0.299	0.000588	0.0329	8.33	0.896	0.848	0.991
$2\times10^{5.}$	0.776	0.000783	0.0183	2.31	0.921	0.867	0.986
$2\times10^{5.5}$	1.71	0.00118	0.0158	1.22	0.918	0.846	0.982
$2\times10^{6.}$	0.972	0.00269	0.0266	1.49	0.945	0.886	0.985
$2\times10^{6.5}$	0.896	0.00637	0.0441	1.74	0.960	0.908	0.987
$2\times10^{7.}$	0.935	0.0170	0.0858	2.35	0.972	0.928	0.988

Table 6.12: A similar table as above for the test parameter ψ_7. Also listed are the correlation coefficients c^{ij} between the parameters ψ_i and ψ_j, i, j = 0, 2, 7.

$M\,(M_\odot)$	SNR$\times 10^3$	$\Delta\psi_0/\psi_0\%$	$\Delta\psi_2/\psi_2\%$	$\Delta\psi_7/\psi_7\%$	c^{02}	c^{07}	c^{27}
$2\times10^{3.}$	0.0148	0.000297	0.276	1120	−0.874	0.951	−0.954
$2\times10^{3.5}$	0.0437	0.000227	0.0681	130.	0.791	−0.576	−0.935
$2\times10^{4.}$	0.115	0.000390	0.0252	20.6	0.841	−0.649	−0.929
$2\times10^{4.5}$	0.299	0.000456	0.0133	4.50	0.864	−0.731	−0.944
$2\times10^{5.}$	0.776	0.000632	0.00916	1.42	0.904	−0.785	−0.943
$2\times10^{5.5}$	1.71	0.000958	0.00825	0.868	0.907	−0.755	−0.935
$2\times10^{6.}$	0.972	0.00219	0.0148	1.45	0.938	−0.824	−0.955
$2\times10^{6.5}$	0.896	0.00517	0.0253	2.04	0.956	−0.860	−0.964
$2\times10^{7.}$	0.935	0.0138	0.0505	3.17	0.970	−0.892	−0.970

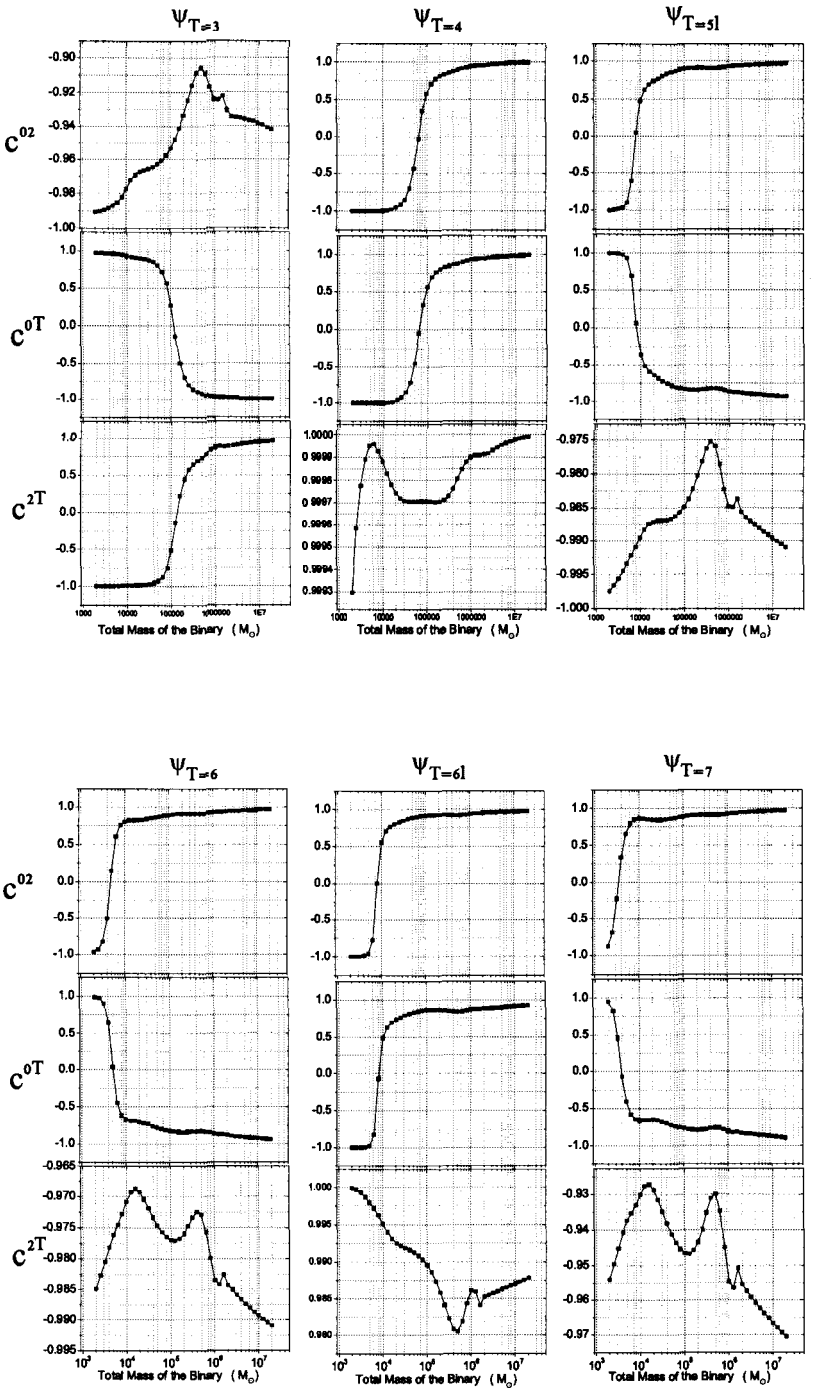

Figure 6.6: Plot showing the variation of the correlation coefficients c^{iT} for LISA with the total mass of the binary. The cosmological model used is (R, $= 0, \Omega_M = 0.3$ and $\Omega_\Lambda = 0.7$) and the redshift is $z = 1$. The waveform model corresponds to the pattern averaged case. c^{iT} is the correlation coefficient between ψ_i, i = 0, 2 and the test parameter ψ_T, T = 6, 6l, 7.

Table 6.13: Variation with total binary mass M of SNR, the relative errors in the A , ψ_0, ψ_2 and ψ_3 for LISA when the test parameter is ψ_3. The cosmologicai model used is ($\Omega_\kappa = 0$, $\Omega_M = 0.3$ and $\Omega_\Lambda = 0.7$) and the redshift is z = 1. The waveform model includes the orientation of the source. The orientation of the source is chosen to be $(\cos\bar{\theta}_S, \bar{\phi}_S, \cos\bar{\theta}_L, \bar{\phi}_L)$ = (09, 2, –0.8, –5). Also listed are the correlation coefficients $c^{ij} = c^{ji}$ between parameters ψ_i and ψ_j, i, j = 0, 2, 3. $c^{\mathcal{A}k}$ is the correlation coefficient between parameters A and ψ_k.

$M\,(M_\odot)$	SNR $\times 10^3$	$\Delta\mathcal{A}/\mathcal{A}\%$	$\Delta\psi_0/\psi_0\%$	$\Delta\psi_2/\psi_2\%$	$\Delta\psi_3/\psi_3\%$	$c^{\mathcal{A}0}$	$c^{\mathcal{A}2}$	$c^{\mathcal{A}3}$	c_{02}	c_{03}	c_{23}
$2\times10^{3.}$	0.0246	1690	0.00436	0.852	1.67	–0.0138	0.00873	–0.00324	–0.991	0.974	–0.995
$2\times10^{3.5}$	0.0777	1080	0.00280	0.316	0.441	–0.338	0.316	–0.284	–0.983	0.949	–0.990
$2\times10^{4.}$	0.186	1390	0.00170	0.111	0.101	–0.323	0.368	–0.347	–0.956	0.857	–0.966
$2\times10^{4.5}$	0.465	768.	0.00126	0.0455	0.0198	–0.242	0.237	–0.133	–0.925	0.544	–0.791
$2\times10^{5.}$	1.19	397.	0.00123	0.0225	0.0106	–0.390	0.303	0.376	–0.892	–0.826	0.630
$2\times10^{5.5}$	2.64	249.	0.00165	0.0184	0.0154	–0.451	0.256	0.427	–0.853	–0.940	0.836
$2\times10^{6.}$	1.50	196.	0.00384	0.0337	0.0331	–0.430	0.215	0.376	–0.902	–0.969	0.919
$2\times10^{6.5}$	1.39	176.	0.00898	0.0540	0.0717	–0.383	0.163	0.303	–0.921	–0.978	0.954
$2\times10^{7.}$	1.45	171.	0.0241	0.0952	0.174	–0.273	0.0649	0.185	–0.939	–0.986	0.970

Table 6.14: A similar table as above for the test parameter is ψ_4.

$M\,(M_\odot)$	SNR $\times 10^3$	$\Delta\mathcal{A}/\mathcal{A}\%$	$\Delta\psi_0/\psi_0\%$	$\Delta\psi_2/\psi_2\%$	$\Delta\psi_4/\psi_4\%$	$c^{\mathcal{A}0}$	$c^{\mathcal{A}2}$	$c^{\mathcal{A}4}$	c_{02}	c_{04}	c_{24}
$2\times10^{3.}$	0.0246	1690	0.0123	3.98	192.	0.00642	–0.00736	–0.00615	–0.999	–1.00	1.00
$2\times10^{3.5}$	0.0777	1030	0.00594	1.82	89.6	0.136	–0.143	–0.141	–0.998	–0.999	1.00
$2\times10^{4.}$	0.186	1340	0.000867	0.342	16.1	0.321	–0.276	–0.276	–0.887	–0.897	1.00
$2\times10^{4.5}$	0.465	767.	0.000403	0.137	6.09	–0.0534	–0.243	–0.241	0.101	0.0811	1.00
$2\times10^{5.}$	1.19	401.	0.000656	0.0988	4.18	–0.413	–0.360	–0.355	0.704	0.693	1.00
$2\times10^{5.5}$	2.64	252.	0.00136	0.136	5.69	–0.494	–0.333	–0.328	0.851	0.845	1.00
$2\times10^{6.}$	1.50	194.	0.00395	0.301	12.4	–0.393	–0.229	–0.224	0.941	0.938	1.00
$2\times10^{6.5}$	1.39	172.	0.0141	0.801	32.7	–0.134	–0.0205	–0.0173	0.981	0.980	1.00
$2\times10^{7.}$	1.45	186.	0.0476	2.21	89.8	0.334	0.409	0.411	0.992	0.992	1.00

Table 6.15: Variation with total binary mass M of SNR, the relative errors in the $\mathcal{A}, \psi_0, \psi_2$ and ψ_{5l} for LISA when the test parameter is ψ_{5l}. The cosmological model used is ($\Omega_\kappa = 0$, $\Omega_M = 0.3$ and $\Omega_\Lambda = 0.7$) and the redshift is z = 1. The waveform model includes the orientation of the source. The orientation of the source is chosen to be $(\cos\bar{\theta}_S, \bar{\phi}_S, \cos\bar{\theta}_L, \bar{\phi}_L)$ = (09, 2, −0.8, −5). Also listed are the correlation coefficients $c^{ij} = c^{ji}$ between parameters ψ_i and ψ_j, i, j = 0, 2, 51. $c^{\mathcal{A}k}$ is the correlation coefficient between parameters $\mathcal{A}$ and ψ_k.

$M\,(M_\odot)$	SNR $\times 10^3$	$\Delta\mathcal{A}/\mathcal{A}\%$	$\Delta\psi_0/\psi_0\%$	$\Delta\psi_2/\psi_2\%$	$\Delta\psi_{5l}/\psi_{5l}\%$	$c^{\mathcal{A}0}$	$c^{\mathcal{A}2}$	$c^{\mathcal{A}5l}$	c_{02}	c_{05l}	c_{25l}
$2\times10^{3.}$	0.0246	1690	0.00213	1.12	59.4	0.0326	−0.0352	0.0302	−0.990	0.998	−0.996
$2\times10^{3.5}$	0.0777	1050	0.000314	0.224	8.97	−0.0561	−0.275	0.251	0.0306	0.0795	−0.990
$2\times10^{4.}$	0.186	1340	0.000495	0.0659	1.86	−0.0469	−0.273	0.277	0.714	−0.615	−0.984
$2\times10^{4.5}$	0.465	762.	0.000564	0.0274	0.530	−0.172	−0.217	0.207	0.768	−0.678	−0.984
$2\times10^{5.}$	1.19	395.	0.000728	0.0172	0.226	−0.393	−0.341	0.304	0.813	−0.736	−0.983
$2\times10^{5.5}$	2.64	250.	0.00112	0.0161	0.173	−0.497	−0.351	0.279	0.821	−0.731	−0.980
$2\times10^{6.}$	1.50	196.	0.00260	0.0314	0.317	−0.506	−0.318	0.250	0.890	−0.830	−0.988
$2\times10^{6.5}$	1.39	177.	0.00644	0.0578	0.512	−0.454	−0.270	0.205	0.931	−0.885	−0.991
$2\times10^{7.}$	1.45	171.	0.0184	0.124	0.944	−0.329	−0.170	0.111	0.962	−0.930	−0.993

Table 6.16: A similar table as above for the test parameter is ψ_6.

$M\,(M_\odot)$	SNR $\times 10^3$	$\Delta\mathcal{A}/\mathcal{A}\%$	$\Delta\psi_0/\psi_0\%$	$\Delta\psi_2/\psi_2\%$	$\Delta\psi_6/\psi_6\%$	$c^{\mathcal{A}0}$	$c^{\mathcal{A}2}$	$c^{\mathcal{A}6}$	c_{02}	c_{06}	c_{26}
$2\times10^{3.}$	0.0246	1690	0.000554	0.479	261.	0.0344	−0.0382	0.0281	−0.912	0.966	−0.981
$2\times10^{3.5}$	0.0777	1050	0.000379	0.114	32.0	−0.193	−0.274	0.237	0.701	−0.563	−0.973
$2\times10^{4.}$	0.186	1330	0.000503	0.0363	5.16	−0.0310	−0.235	0.245	0.781	−0.651	−0.966
$2\times10^{4.5}$	0.465	758.	0.000532	0.0154	1.17	−0.149	−0.199	0.189	0.774	−0.660	−0.972
$2\times10^{5.}$	1.19	393.	0.000667	0.00996	0.428	−0.377	−0.337	0.300	0.798	−0.712	−0.979
$2\times10^{5.5}$	2.64	249.	0.00101	0.00897	0.282	−0.500	−0.374	0.301	0.806	−0.704	−0.977
$2\times10^{6.}$	1.50	196.	0.00224	0.0173	0.481	−0.535	−0.355	0.282	0.871	−0.801	−0.986
$2\times10^{6.5}$	1.39	177.	0.00535	0.0313	0.725	−0.504	−0.319	0.248	0.915	−0.861	−0.990
$2\times10^{7.}$	1.45	172.	0.0148	0.0661	1.25	−0.400	−0.233	0.168	0.953	−0.915	−0.993

Table 6.17: Variation with total binary mass M of SNR, the relative errors in the 34, ψ_0, ψ_2 and ψ_{61} for LISA when the test parameter is ψ_{61}. The cosmological model used is ($\Omega_\kappa = 0$, $\Omega_M = 0.3$ and $\Omega_\Lambda = 0.7$) and the redshift is z = 1. The waveform model includes the orientation of the source. The orientation of the source is chosen to be $(\cos\bar{\theta}_S, \bar{\phi}_S, \cos\bar{\theta}_L, \bar{\phi}_L)$ = (09, 2, –0.8, –5). Also listed are the correlation coefficients $c^{ij} = c^{ji}$ between parameters ψ_i and ψ_j, i, j = 0, 2, 61. $c^{\mathcal{A}k}$ is the correlation coefficient between parameters $\mathcal{A}$ and ψ_k.

$M\,(M_\odot)$	SNR $\times 10^3$	$\Delta\mathcal{A}/\mathcal{A}\%$	$\Delta\psi_0/\psi_0\%$	$\Delta\psi_2/\psi_2\%$	$\Delta\psi_{61}/\psi_{61}\%$	$c^{\mathcal{A}0}$	$c^{\mathcal{A}2}$	$c^{\mathcal{A}61}$	c_{02}	c_{061}	c_{261}
$2\,x\,10^{3.}$	0.0246	1690	0.00860	4.00	8110	0.00763	−0.00843	−0.00716	−0.999	−1.00	1.00
$2\,x\,10^{3.5}$	0.0777	1070	0.000337	0.381	387.	0.0519	−0.329	−0.317	−0.320	−0.373	0.998
$2\,x\,10^{4.}$	0.186	1360	0.000545	0.0775	38.1	−0.113	−0.318	−0.321	0.773	0.711	0.992
$2\,x\,10^{4.5}$	0.465	764.	0.000596	0.0272	6.57	−0.188	−0.230	−0.223	0.801	0.736	0.990
$2\,x\,10^{5.}$	1.19	396.	0.000736	0.0151	1.84	−0.395	−0.347	−0.317	0.825	0.763	0.988
$2\,x\,10^{5.5}$	2.64	250.	0.00109	0.0127	0.941	−0.499	−0.362	−0.297	0.824	0.741	0.983
$2\,x\,10^{6.}$	1.50	196.	0.00244	0.0227	1.22	−0.519	−0.337	−0.267	0.885	0.822	0.987
$2\,x\,10^{6.5}$	1.39	177.	0.00582	0.0394	1.48	−0.482	−0.298	−0.226	0.924	0.871	0.989
$2\,x\,10^{7.}$	1.45	172.	0.0161	0.0806	2.10	−0.373	−0.210	−0.139	0.957	0.917	0.990

Table 6.18: A similar table as above for the test parameter is ψ_7.

$M\,(M_\odot)$	SNR $\times 10^3$	A	$\Delta\psi_0/\psi_0\%$	$\Delta\psi_2/\psi_2\%$	$\Delta\psi_7/\psi_7\%$	$c^{\mathcal{A}0}$	$c^{\mathcal{A}2}$	$c^{\mathcal{A}7}$	c_{02}	c_{07}	c_{27}
$2\times 10^{3.}$	0.0246	1690	0.000226	0.293	941.	0.0387	-0.0431	0.0271	-0.590	0.772	-0.949
$2\times 10^{3.5}$	0.0777	1040	0.000389	0.0747	109.	-0.185	-0.265	0.211	0.783	-0.592	-0.933
$2\times 10^{4.}$	0.186	1320	0.000480	0.0251	16.4	0.00755	-0.194	0.211	0.792	-0.601	-0.924
$2\times 10^{4.5}$	0.465	755.	0.000501	0.0108	3.28	-0.128	-0.181	0.167	0.768	-0.591	-0.935
$2\times 10^{5.}$	1.19	390.	0.000623	0.00726	1.06	-0.361	-0.331	0.275	0.783	-0.644	-0.949
$2\times 10^{5.5}$	2.64	248.	0.000938	0.00650	0.635	-0.498	-0.390	0.274	0.796	-0.622	-0.937
$2\times 10^{6.}$	1.50	196.	0.00202	0.0123	1.12	-0.552	-0.382	0.263	0.856	-0.728	-0.960
$2\times 10^{6.5}$	1.39	178.	0.00473	0.0221	1.66	-0.537	-0.355	0.236	0.903	-0.799	-0.968
$2\times 10^{7.}$	1.45	173.	0.0128	0.0465	2.71	-0.448	-0.280	0.168	0.945	-0.869	-0.975

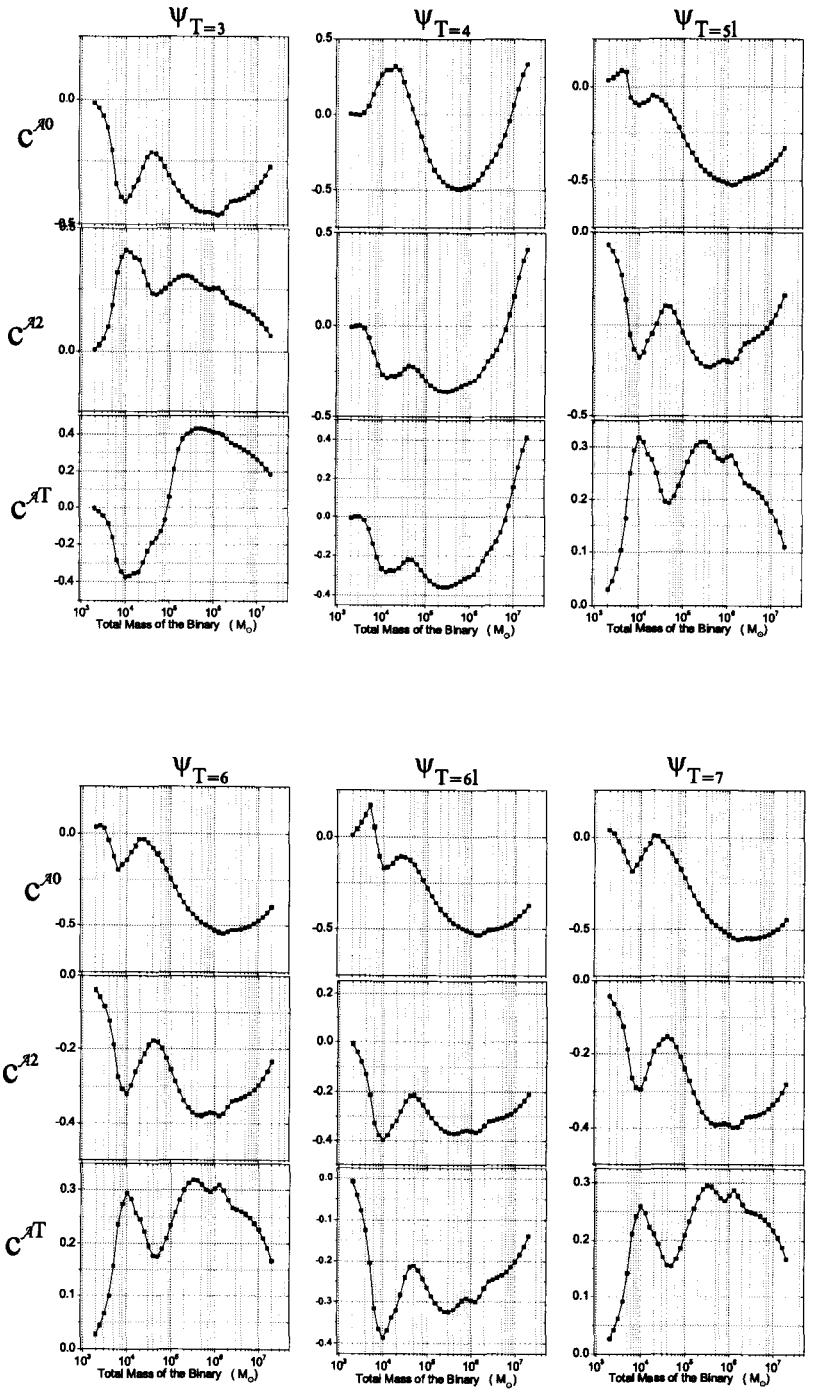

Figure 6.7: Plot showing the variation of the correlation coefficients $c^{\mathcal{A}T}$ for LISA with the total mass of the binary.The cosmological model used is ($\Omega_\kappa = 0$, $\Omega_M = 0.3$ and $\Omega_\Lambda = 0.7$) and the redshift is $z = 1$. The waveform model includes the orientation of the source. The orientation of the source is chosen to be $(\cos\bar{\theta}_S, \bar{\phi}_S, \cos\bar{\theta}_L, \bar{\phi}_L) = (0.9, 2, -0.8, -5)$. $c^{\mathcal{A}T}$ is the correlation coefficient between $\mathcal{A}$ and the test parameter ψ_T, T=3, 4, 5l, 6, 6l, 7.

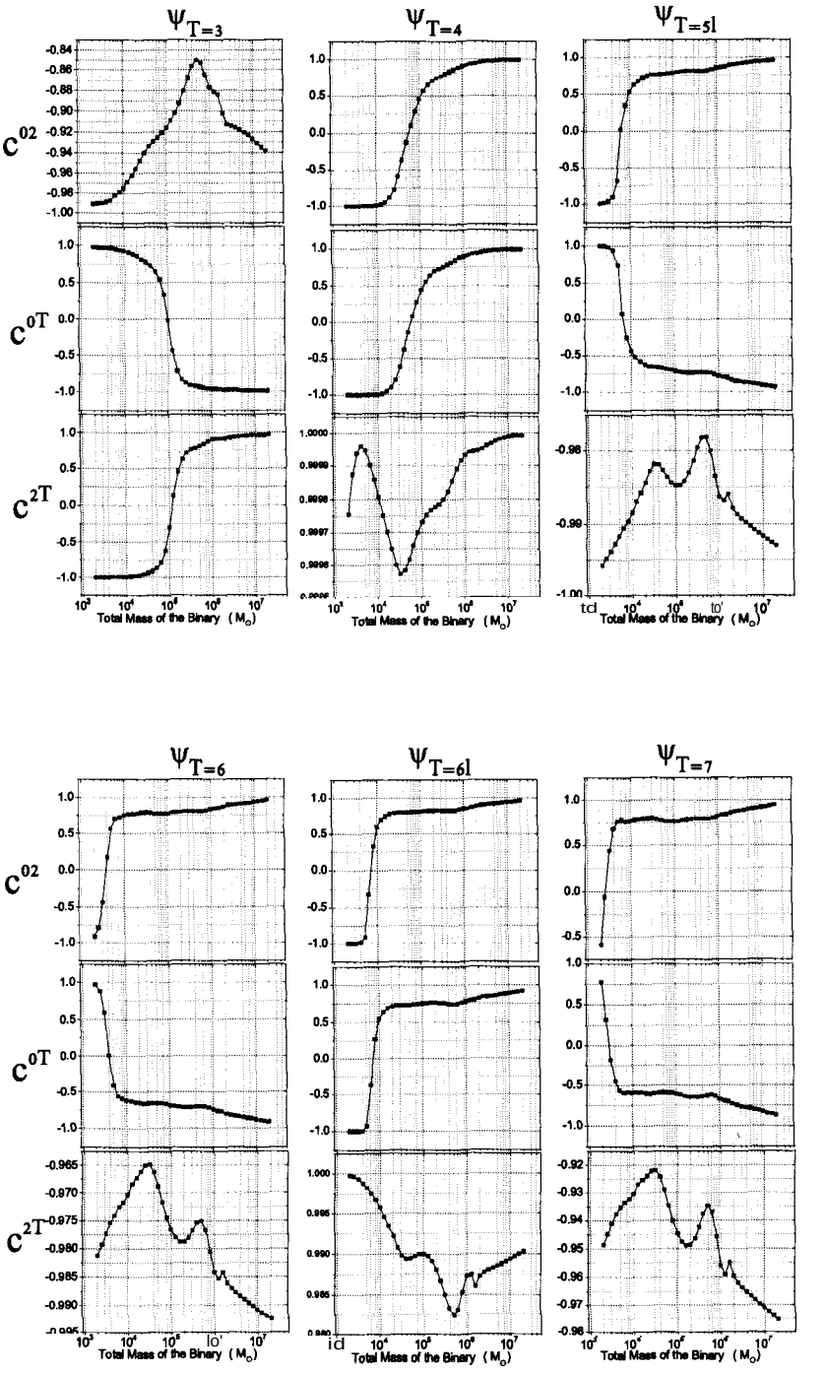

Figure *6.8:* Plot showing the variation of the correlation coefficients c^{iT} for LISA with the total mass of the binary.The cosmological model used is ($\Omega_\kappa = 0$, $\Omega_M = 0.3$ and $\Omega_\Lambda = 0.7$) and the redshift is $z = 1$. The waveform model includes the orientation of the source. The orientation of the source is chosen to be $(\cos\bar{\theta}_S, \bar{\phi}_S, \cos\bar{\theta}_L, \bar{\phi}_L) = (0.9, 2, -0.8, -5)$. c^{iT} is the correlation coefficient between $i = 0$, 2 and the test parameter ψ_T, T=3, 4, 51, 6, 61, 7.

behaviour. Recall that the PN terms in the Fourier phase are given by $\psi_k f^{(k-5)/3}$. When k = 5, there is no dependence on the frequency and when k = 4 the term varies very slowly as $f^{-1/3}$. Therefore, terms close to k = 5 are likely to suffer from large variances since the frequency dependence of the corresponding term is weak. Although one might expect ψ_6 to also suffer from large relative errors, the fact that in this case the term increases with frequency as $f^{1/3}$, makes it a more important term than ψ_4. We also observe that ψ_4 has significantly larger covariances with ψ_2, (see Tables 6.2, 6.8 and 6.14), which adds to its poor determination.

6.5 Representation in the m_1-m_2 plane

In Fig. [6.10]and [6.9] , we have depicted the power of the proposed test in the m_1-m_2 plane. We present for EGO and LISA the uncertainty contours, with 1-σ error bars, associated with the different test parameters $\psi_T = \psi_3, \psi_4, \psi_{5l}, \psi_6, \psi_{6l}, \psi_7$ in the m_1-m_2 plane, when ψ_0 and ψ_2 are used to parametrize the waveform. For EGO the source corresponds to a $(10, 10)M_\odot$ black hole binary at a luminosity distance D_L = 200 Mpc. For LISA the corresponding source is a $(10^6, 10^6)M_\odot$ supermassive black hole binary at a redshift of $z = 1$ observed in its last year before merger.

The region in the $m_1 - m_2$ plane for a binary of total mass M_0 corresponding to the parameter ψ_k is determined as follows. It is given by $R_k(m_1, m_2;\ (\psi_k)|_{M=M_0} - \delta_k))=0$, where $-\Delta\psi_k|_{M=M_0} \leq \delta_k \leq \Delta\psi_k|_{M=M_0}$. In the above $\Delta\psi_k$ corresponds to the estimated errors in ψ_k for a particilar detector and particular source of total mass M_0. Normally, there is an 'allowed' region in the $m_1 - m_2$ plane associated with each of the ψ_k's. However, one boundary for ψ_4 does not appear in the plot; the region determined by ψ_4 is almost the whole area in the figure. This implies that the test using ψ_4 is a poor one and thus the determination of m_1 and m_2 using ψ_4 not recommended. The test parameter ψ_3 corresponds to the smallest region in the m_1-m_2 plane relative to the other parameters. The 1-σ uncertainty in ψ_3 is smaller than the thickness of the line. The allowed region corresponding to ψ_{5l} has only one boundary. In this case, the equation determining the other boundary has no real solution. Finally, the parameter ψ_{6l} is much better determined by LISA than EGO, as one would expect. These figures are an explicit demonstration of the efficacy of the proposed test and the accuracy with which the future GW observations of BH binaries by EGO and LISA and in the more immediate future, Advanced LIGO, can test GR in its strong field regime.

As mentioned earlier, the spin and angular parameters add a lot of structure to the waveform which contain additional information that can be extracted and more tests conducted. Covariance between the old and new parameters is likely to increase the error boxes but the tests become more demanding as a result of seeking consistency amongst a greater number of parameters. Future studies should look into the more general case incorporating the

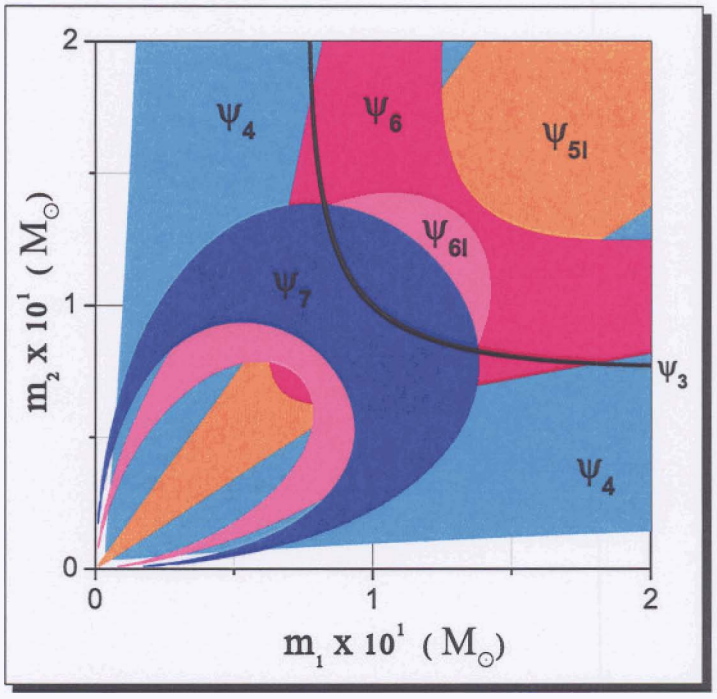

Figure 6.9: Plot showing the regions in the m_1-m_2 plane that correspond to 1-σ uncertainties in the test parameters $\psi_T = \psi_3, \psi_4, \psi_{51}, \psi_6, \psi_{61}, \psi_7$ for a (10, 10)$M_\odot$, (i.e. $M_0 = 20\,M_\odot$), **black hole binary at a** luminosity **distance** $D_L = 200$ Mpc observed using EGO. **Normally, there is an 'allowed' region in the** $m_1 - m_2$ **plane associated** with each **of the** ψ_k**'s. However, one** boundary **for** ψ_4 **does not appear in the plot; the region** determined **by** ψ_4 **is almost the whole area in the figure.** This quantifies **how bad the** test **of** ψ_4 actually **is and** thus **how bad will be the** determination **of** m_1 **and** m_2 **wing** ψ_4**. The** test **parameter** ψ_3 **corresponds to** the **smallest region in the** m_1-m_2 **plane relative to the other parameters. Finally,** the **allowed** region **corresponding to** ψ_{51} **has only** one **boundary. In this case,** the **equation determining** *the* **other boundary has no real solution.**

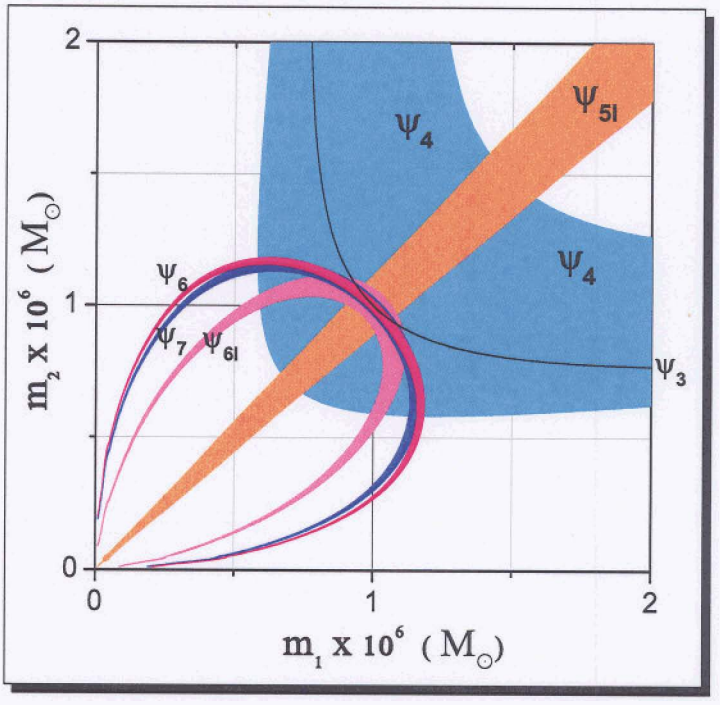

Figure 6.10: Plot showing the regions in the m_1-m_2 plane that correspond to 1-σ uncertainties in the test parameters $\psi_T = \psi_3, \psi_4, \psi_{5l}, \psi_6, \psi_{6l}, \psi_7$ for a $(10^6, 10^6)M_\odot$, (i.e. $M_0 = 2 \times 10^6\, M_\odot$), supermassive black hole binary at a redshift of $z = 1$ as observed for a year before merger by LISA, Normally, there is an 'allowed' region in the $m_1 - m_2$ plane associated with each of the ψ_k's. However, one boundary for ψ_4 does not appear in the plot; the region determined by ψ_4 is almost the whole area in the figure. This quantifies how bad the test of ψ_4 actually is and thus how bad will be the determination of m_1 and m_2 using ψ_4. The test parameter ψ_3 corresponds to the smallest region in the m_1-m_2 plane relative to the other parameters. The 1-σ uncertainty in ψ_3 is smaller than the thickness of the line. Finally, the allowed region corresponding to ψ_{5l} has only one boundary. In this case, the equation determining the other boundary has no real solution.

effects of spin and systematic effects of orbital eccentricity that could affect the tests, and more interestingly, go beyond the restricted waveform approximation by incorporating the amplitude corrections [110] to the GW phasing.

6.6 Bounds on Compton wavelength of the graviton using the current proposal

We conclude by discussing the extent to which we can extend the current proposal to discriminate between different theories of gravity such as massive graviton theories and scalar-tensor theories [214, 136, 217]. The limitations of GW phasing to quantitatively discriminate between alternate theories of gravity has been critically discussed in [211] and should be kept in mind. For massive graviton theories the 1PN phasing term ψ_2 is different and also involves the Compton wavelength of the graviton A.

We adopt the following procedure to calculate the bounds on the mass of the graviton. The presence of a massive graviton modifies the 1PN terms of the phasing formula which for our analysis can be viewed as

$$\psi_2 = \psi_2^{\rm GR} + \psi_2^{\rm MG}\,, \tag{6.9}$$

$$\text{where,}\quad \psi_2^{\rm GR} = \frac{3715}{(32256} + \frac{55}{384}\,\nu\Big)\frac{1}{\pi\,\nu\,M}\,, \tag{6.10}$$

and $\psi_2^{\rm MG}$ the leading correction due to the effect of the massive graviton is given by

$$\psi_2^{\rm MG} = -\frac{c^2\,\pi\,D}{(1+z)\lambda_g^2}\,. \tag{6.11}$$

$\psi_2^{\rm MG}$ will alter the arrival time of the waves of a given frequency and depends only on the size of the graviton Compton wavelength A, and on a distance parameter D which is defined as [196, 195]

$$\boldsymbol{D} = \frac{c\,(1+z)}{H_0}\int_0^z \frac{dz'}{(1+z')^2\,[\Omega_M(1+z')^3+\Omega_\Lambda]^{1/2}}\,. \tag{6.12}$$

Recall that D is *not* the conventional cosmological distance measure, D_L [195].

Using ψ_0 and ψ_3 as basic variables and ψ_2 as a test, we find that bounds can be set on the value of A, modulo the neglect of uncomputed higher PN order corrections in the theory. For a BH binary of total mass 2 x $10^6\,M_\odot$ at the luminosity distance D_L = 6612.2 Mpc, that is, (z = 1 and D = 3523.2 Mpc) in the LISA band, one obtains the values $\psi_2^{\rm GR}$ = 0.0195 and $\psi_2^{\rm MG} \simeq -\frac{5.1}{\left(\lambda_g/(10^{14}\,\mathrm{Km})\right)^2}$. From the results in Sec. 6.4.4, the error in estimating ψ_2 is $\Delta\psi_2 = \frac{0.0267}{\rho(z)}$. The massive graviton model can be distinguished from GR if $\psi_2^{\rm MG} \geq \Delta\psi_2$, say,

$\psi_2^{\rm MG} = 10 \times \Delta\psi_2$, which we adopt as our criterion. For the system considered, we use our estimate of $\Delta\psi_2$ to obtain the value of A, that satisfies our criterion. Any massive graviton theory of this type, with λ_g less than or equal to this value can be distinguished from GR by the proposed test.

Given the theoretical status of the phasing formula in the massive graviton case, this choice we implement is the most convenient one at present. Our analyses for the alternative gravity case is modulo uncomputed higher order effects in these alternative theories. In a more complete theory ψ_3 could in general depend on the Compton wavelength as well and there would be not much rationale behind the choice proposed. One could then use ψ_0 and ψ_2 as basic variables and ψ_3 as a test, as before. Using EGO, which will observe stellar mass BH coalescences, we can set a bound on A, to be 1.3×10^{13} km whereas with LISA the bounds are as high as 7.12×10^{16} km.

Scalar-tensor theories like Brans-Dicke theory, which predicts dipolar GW emission, have additional leading terms in the the phasing formula at a PN order lower than in GR. But the dipole GW emission is more important for asymmetric binaries than it is for equal mass systems. However, for such systems spin effects are also expected to play a crucial role. The present chapter deals with only non-spinning binaries and we will have to postpone the questions relating to dipolar radiation including spin effects to a future analysis. Once again, these tests will be limited by the uncomputed higher order PN contributions in the Brans-Dicke theory.

6.7 Summary

Based on the analyses of the previous sections, we can finally provide an executive summary of the results that we have discovered in this chapter. In Table 6.7 the relative errors $\Delta\psi_k/\psi_k$ is summarised for the Advanced LIGO, EGO and LISA cases respectively. The relative errors have been calculated for the total binary mass of $20M_\odot$ and $2 \times 10^6 M_\odot$ at luminosity distance $D_L = 0.200$ Gpc and $D_L = 6.61223$ Gpc ($z = 1$) for Advanced-LIGO/EGO and LISA respectively. The corresponding values of SNR are about **38,** 144 and 1000-1500 respectively. In the case of LISA the two values corresponds to the averaged waveform pattern and to the waveform including the orientation pattern. With the prototypical black hole binary at a typical distance chosen here, Advanced-LIGO can only hope to test ψ_3, ψ_{5l}, and ψ_6. With EGO, however, all the ψ_k's, except ψ_4, can be tested. The LISA detector can test all the ψ_k's with excellent accuracy with a supermassive black hole binary of total mass $2 \times 10^6 M_\odot$ at a cosmological redshift $z = 1$.

In Table 6.20 the minimum SNR required in this proposal to test various PN order coefficients are summarized for Advanced LIGO, EGO and LISA detectors. From the Table one

can see that with a prototypical 2 x $10M_{\odot}$ BBH, EGO only requires a SNR of 20 to test ψ_3, ψ_{5l}, ψ_{6l}, and ψ_7. LISA can do much better. With its SMBH prototypical source it can test all the PN coefficients ψ_k using this scheme at a SNR of 120-200. We also provide an alternative presentation *viz* the maximum distance at which the source can be located and yet lead to a feasible test of the particular PN coefficient in the phasing formula.

6.8 Testing PN gravity: Future prospects

We conclude with a few directions in which this present work can be extended in the furure.

- In the future we intend to develop the proposed test in such a way that this can be implemented with the real data from LIGO/VIRGO/LISA. The assumptions with which we work at present could be relaxed and the test generalized.

- The effect of spin which we have neglected in the present work, can be included especially with the 2.5PN spin-orbit term in the phasing being completed recently [218, 219].

- The effect of orbital eccentricity could be significant, at least for many of the anticipated LISA sources. Though including eccentricity in a complete way may be a hard task, one can use the treatment in [220] which is applicable for small eccentricities to understand the effect of its inclusion.

- Another obvious modification is to go beyond the inspiral waveform and include available information about the merger phase. Though one might have to wait till the numerical simulations succeed in their hard task of computing the merger waveforms using numerical relativity, as a first step, one can try modelling the merger phase using approaches like the effective one body formalism [24].

- Recently Luna and Sintes [221] noted that adding the ringdown information to the inspiral waveform will improve the parameter estimation of the mass parameters compared to that in Ref [215]. Though a similar study could be performed in the present context, there would be conceptual issues since the masses appearing in the ringdown and inspiral waveforms are not the same.

- Restricted PN waveforms will only bring new variety (higher harmonics) without increasing the number of parameters; a full test should definitely use the full waveform. One should thus investigate in detail the effect of the full waveform [43, 110, 222] (as opposed to the restricted waveform used here). The additional information about

Table 6.19: The following table summarizes the central results of this chapter. It lists the values of the relative errors $\Delta\psi_k/\psi_k$ for k={0, 2, T} where T labels the test parameter. The table is horizontally partitioned into 6 sub-tables, corresponding to the six possible test parameters at 3.5PN order. Every sub-table has three rows, the first two rows corresponding to the basic chosen variables, (in this work we choose ψ_0 and ψ_2), and the third row corresponding to the test parameter ψ_T. The values of the relative errors have been calculated for the total binary mass of $20M_\odot$ and $2\times10^6M_\odot$ at luminosity distance $D_L = 0.200$ Gpc and $D_L = 6.61223$ Gpc ($z = 1$) for ground based detectors (Advanced-LIGO and EGO) and space based detector (LISA) respectively, as shown in the table. The corresponding values of SNR are listed. In the case of LISA there are two columns: one corresponds to the averaged waveform pattern and the other to the waveform including the orientation pattern. With the prototypical black hole binary at a typical distance chosen here, Advanced-LIGO can only hope to test ψ_0, ψ_2, ψ_3, ψ_{5l}, and $6. With EGO however, all the ψ_k's, except ψ_4, can be tested. The LISA detector can test all the ψ_k's with excellent accuracy using a supennassive black hole binary of total mass 2 x $10^6M_\odot$ at a cosmological redshift $z = 1$.

	$M = 20M_\odot$ $D_L = 0.200$ Gpc		M = $2\times10^6M_\odot$ $D_L = 6.61223$ Gpc, $z = 1$	
	Advanced LIGO	EGO	LISA **(Without pattern)**	LISA (With **pattern)**
SNR≡ ρ	37.5313	143.923	971.629	1499.26
$\Delta\psi_0/\psi_0$	0.013137	0.00063028	0.000043626	0.000038441
$\Delta\psi_2/\psi_2$	0.040054	0.0039177	0.00040555	0.00033733
$\Delta\psi_3/\psi_3$	0.079637	0.0043976	0.00035428	0.00033069
$\Delta\psi_0/\psi_0$	0.026753	0.00087828	0.000039616	0.000039470
$\Delta\psi_2/\psi_2$	1.0303	0.043544	0.0029701	0.0030124
$\Delta\psi_4/\psi_4$	41.612	1.7786	0.12312	0.12444
$\Delta\psi_0/\psi_0$	0.010391	0,00044110	0.000028807	0.000026011
$\Delta\psi_2/\psi_2$	0.056181	0.0038843	0.00036579	0.00031403
A ψ_{5l}	0.41028	0.037013	0.0038650	0.0031684
$\Delta\psi_0/\psi_0$	0.0082127	0.00036098	0.000024594	0.000022372
$\Delta\psi_2/\psi_2$	0.029740	0.0021116	0.00020513	0.00017274
$\Delta\psi_6/\psi_6$	0.94272	0.28855	0.0059558	0.0048112
$\Delta\psi_0/\psi_0$	0.0063744	0.00033679	0.000026946	0.000024382
$\Delta\psi_2/\psi_2$	0.013845	0.0017404	0.00026571	0.00022679
$\Delta\psi_{6l}/\psi_{6l}$	2.7794	0.098413	0.014930	0.012201
$\Delta\psi_0/\psi_0$	0.0069857	0.00031177	0.000021906	0.000020221
$\Delta\psi_2/\psi_2$	0.020836	0.0014859	0.00014789	0.00012303
$\Delta\psi_7/\psi_7$	1.1504	0.12867	0.014483	0.011228

Table 6.20: The table shows the minimum value of signal to noise ratio (SNR) ρ required to test the PN coefficient ψ_k (*i.e.* $\Delta\psi_k/\psi_k \sim 1$ for k={0,2,T}={0,2,3}, {0,2,4},...,{0,2,7}) with a prototypical black hole binary of mass $2 \times 10 M_\odot$ for ground based detectors (Advanced-LIGO, EGO) and supermassive black hole binary of mass $2 \times 10^6 M_\odot$ for space based detector (LISA) respectively. The table is divided into 6 sub-tables. Every sub-table has three rows, one each for ψ_0, ψ_2, ψ_T where ψ_0 and ψ_2 are the chosen fundamental variables and ψ_T is the test parameter. From the table one can conclude that with a $2 \times 10 M_\odot$ black hole binary EGO only requires a SNR of 20 to test $\psi_3, \psi_{5l}, \psi_{6l}$ and ψ_7, if one uses the scheme proposed here considering two basic variables and a test parameter. LISA using a supermassive black hole binary can test ***all*** the ψ_k's if the SNR is about 120 using the pattern averaged waveform and 190 using the orientation waveform.

	M = $20 M_\odot$		M = $2 \times 10^6 M_\odot$	
	Advanced LIGO	EGO	**LISA (Without pattern)**	LISA **(With pattern)**
ψ_0	0.4931	0.09071	0.04239	0.05763
ψ_2	1.503	0.5638	0.3940	0.5057
ψ_3	2.989	0.6329	0.3442	0.4958
ψ_0	1.004	0.1264	0.03849	0.05918
ψ_2	38.67	6.267	2.886	4.516
ψ_4	1562.	256.0	119.6	186.6
ψ_0	0.3900	0.06348	0.02799	0.03900
ψ_2	2.109	0.5590	0.3554	0.4708
ψ_{5l}	15.40	5.327	3.755	4.750
ψ_0	0.3082	0.05195	0.02390	0.03354
ψ_2	1.116	0.3039	0.1993	0.2590
ψ_6	35.38	41.53	5.787	7.213
ψ_0	0.2392	0.04847	**0.02618**	**0.03655**
ψ_2	0.5196	0.2505	0.2582	0.3400
ψ_{6l}	104.3	14.16	14.51	18.29
ψ_0	0.2622	0.04487	0.02128	0.03032
ψ_2	0.7820	0.2138	0.1437	0.1845
ψ_7	43.18	18.52	14.07	16.83

Table 6.21: The following table summarizes the maximum values of luminosity distance D_L in Gpc up to which the test for a particular ψ_k is feasible using a BBH of the total mass $20M_\odot$ for ground based detectors (Advanced-LIGO, EGO) and a SMBBH of total mass 2 x $10^6 M_\odot$ for the space based detector LISA ($\Delta\psi_k/\psi_k \sim 1$ for k={0,2,T}={0,2,3}, {0,2,4},..., {0,2,7}). The table is divided to 5 sub-tables; every sub-table has three rows ψ_0, ψ_2, ψ_T where ψ_0 and ψ_2 are our selected fundamental variables and ψ_T is the test parameter. From the table one can conclude that with a $20M_\odot$ BBH EGO can test for all the ψ_k's except ψ_4 and ψ_6 at D_L = 6.7 Gpc or z = 1. More importantly, with a 2 x $10^6 M_\odot$ SMBBH LISA can test all the ψ_k's at $z = 1$ and even as far as 53 Gpc. Testing GR using only three parameters ψ_0, ψ_2, ψ_T at a time is a powerful test.

	M = $20M_\odot$		M = $2\times10^6 M_\odot$	
	Advanced LIGO	EGO	LISA (Without **pattern)**	LISA (With **pattern)**
ψ_0	15.2238	317.320	151565.	172010.
ψ_2	4.99331	51.0510	16304.4	19601.9
ψ_3	2.51138	45.4798	18663.9	19995.5
ψ_0	7.47581	227.719	166909.	167524.
ψ_2	0.194118	4.59309	2226.28	2194.99
ψ_4	0.00480634	0.112448	53.7058	53.1340
ψ_0	19.2482	453.410	229535.	254207.
ψ_2	3.55990	51.4889	18076.4	21056.2
ψ_5	0.487476	5.40357	1710.78	2086.96
ψ_0	24.3525	554.045	268856.	295556.
ψ_2	6.72495	94.7140	32234.3	38279.6
ψ_6	0.212151	0.693109	1110.21	1374.35
ψ_0	31.3754	593.841	245386.	271193.
ψ_2	14.4455	114.917	24885.4	29155.8
ψ_6	0.0719581	2.03226	442.890	541.951
ψ_0	28.6298	641.498	301852.	327003.
ψ_2	9.59884	134.603	44711.6	53744.8
ψ_7	0.173849	1.55436	456.565	588.930

the masses could make possible more interesting tests [223]. Including PN amplitude corrections is generally expected to improve the tests and this is what would be a follow-up of the present analysis.

- In the LISA case one should eventually deal with the problem in terms of the time delay interferometry variables [224] so as to have close contact with the real LISA situation. Lastly, a careful analysis will have to be done to extend the present proposal to include, in greater detail, the case of alternate theories of gravity, especially the scalar tensor theories like BD theory.

We wish to return to these issues and develop them further in future works.

Bibliography

[1] I. Ciufolini, V. Gorini, U. Moschella and P. Fre, editors, Gravitational Waves (Institute of Physics, (Seriess in High Energy Physics, Cosmology and Gravitation), 2001).

[2] B. F. Schutz, "Gravitational radiation", (2000).

[3] E. E. Flanagan and S. A. Hughes, "The basics of gravitational wave theory", New Journal of Physics 7, 204 (2005).

[4] B. S. Sathyaprakash, "Gravitational Radiation - Observing the Dark and Dense Universe", (2004).

[5] L. P. Grishchuk, V. M. Lipunov, K. A. Postnov, M. E. Prokhorov and B. S. Sathyaprakash, "Gravitational Wave Astronomy: in Anticipation of First Sources to be Detected", Usp. Fiz. Nauk **171**, 3 (2001).

[6] L. P. Grishchuk, V. M. Lipunov, K. A. Postnov, M. E. Prokhorov and B. S. Sathyaprakash, "Gravitational wave astronomy: In anticipation of first sources to be detected", Phys. Usp. 44, 1 (2001).

[7] L. Blanchet, "Gravitational radiation from post-Newtonian sources and inspiralling compact binaries", Living Rev. Rel. 5, 3 (2002).

[8] S. A. Hughes, M. Favata and D. E. Holz, "How black holes get their kicks: radiation recoil in binary black hole mergers", in Growing Black Holes: Accretion in a Cosmological Context, edited by A. Merloni, S. Nayakshin and R. A. Sunyaev, pages 333–339 (2005).

[9] C. M. Will, "Was Einstein Right? Testing Relativity at the Centenary", (2005).

[10] **A.** Abramovici, W. E. Althouse, R. W. P. Drever, Y. Gursel, S. Kawamura, F. J. Raab, D. Shoemaker, L. Sievers, R. E. Spero and K. S. Thorne, "LIGO - The Laser Interferometer Gravitational-Wave Observatory", Science 256, 325 (1992).

[11] E. Coccia, "Gravitational Experiments", World Scientific, Singapore 161 (1995).

[12] M. Cerdonio, "Gravitational Experiments", World Scientific, Singapore **176 (1995).**

[13] http://www.ligo.caltech.edu.

[14] http://www.virgo.infn.it.

[15] http://www.geo600.uni-hannover.de.

[16] tamago.mtk.nao.ac.jp.

[17] http://lisa. jpl.nasa.gov.

[18] R. Takahashi and T. Nakamura, "The Decihertz Laser Interferometer Can Determine the Position of the Coalescing Binary Neutron Stars within an Arcminute a Week before the Final Merging Event to the Black Hole", Astrophys. J. **596, L231 (2003).**

[19] E. S. Phinney, "NASA Mission Concept Study", **(2003).**

[20] B. **F.** Schutz, "Determining the Hubble constant from gravitational wave observations", Nature (London) **323,310 (1986).**

[21] P. Jaranowski, **K.** Kokkatas, A. Krolak and G. Tsegas, "On the estimation of parameters of the gravitational-wave signal from a coalescing binary by a network of detectors", Class. Quantum Grav **13, 1279 (1996).**

[22] C. Cutler and E. Flanagan, "Gravitational waves from merging compact binaries: How accurately can one extract the binary's parameters from the inspiral waveform?', Phys. Rev. D **49, 2658 (1994).**

[23] B. Brügmann, "Numerical Relativity in **3+1** Dimensions", Annalen der Physik **9, 227 (2000).**

[24] A. Buonanno and T. Damour, "Effective one-body approach to general relativistic two-body dynamics, ADM formalism", Phys. Rev. D **59,084006 (1999).**

[25] A. Buonanno and T. Damour, "Transition from inspiral to plunge in binary black hole coalescences", Phys. Rev. D **62,064015 (2000).**

[26] T. Damour, B. R. Iyer and B. S. Sathyaprakash, "A comparison of search templates for gravitational waves from binary inspiral", Phys. Rev. D **63, 044023** (2001), erratum-ibid. **D 72 (2005) 029902.**

[27] E. E. Flanagan and S. A. Hughes, "Measuring gravitational waves from binary black hole coalescences. I. Signal to noise for inspiral, merger, and ringdown", Phys. Rev. D **57,4535 (1998).**

[28] V. Kalogera, C. Kim, D. Lorimer, M. Burgay, N. D'Amico, A. Possenti, R. Manchester, A. Lyne, B. Joshi, M. McLaughlin, M. Kramer, J. Sarkissian and F. Camilo, "The cosmic coalescence rates for double neutron star binaries", Astrophys. J. 601, L179 (2004), erratum, ibid 614, L137 (2004).

[29] L. S. Finn, "Binary inspiral, gravitational radiation, and cosmology", Phys. Rev. D 53, 2878 (1996).

[30] L. P. Grishchuk, V. M. Lipunov, K. A. Postnov, M. E. Prokhorov and B. S. Sathyaprakash, "Gravitational Wave Astronomy: in Anticipation of First Sources to be Detected", Phys. Usp 44, 1 (2001).

[31] W. M. Folkner, editor, Laser *Interferometer* Space Antenna (1998).

[32] B. Allen and J. D. Romano, "Detecting a stochastic background of gravitational radiation: Signal processing strategies and sensitivities", Phys. Rev. D 59, 102001 (1999).

[33] K. S. Thorne, "Gravitational Radiation", in Three hundred years of gravitation, edited by S. Hawking and W. Israel, pages 330–458 (Cambridge University Press, 1987).

[34] T. Damour, B. R. Iyer and B. S. Sathyaprakash, "Frequency-domain P-approximant filters for time-truncated inspiral gravitational wave signals from compact binaries", Phys. Rev. D 62,084036 (2000).

[35] S. V. Dhurandhar and B. F. Schutz, "Filtering coalescing binary signals: Issues concerning narrow banding, thresholds, and optimal sampling", Phys. Rev. D 50, 2390 (1994).

[36] B. J. Owen, "Search templates for gravitational waves from inspiraling binaries: Choice of template spacing", Phys. Rev. D 53,6749 (1996).

[37] L. P. Grishchuk, V. M. Lipunov, K. A. Postnov, M. E. Prokhorov and B. S. Sathyaprakash, "Gravitational Wave Astronomy: in Anticipation of First Sources to be Detected", USP.FIZ.NAUK **171**, 3 (2001).

[38] C. Cutler, L. Finn, E. Poisson and G. Sussman, "Gravitational radiation from a particle in circular orbit around a black hole. II. Numerical results for the nonrotating case", Phys. Rev. D 47, 1511 (1993).

[39] T. Damour, B. R. Iyer and B. S. Sathyaprakash, "Improved filters for gravitational waves from inspiraling compact binaries", Phys. Rev. D 57, 885 (1998).

[40] T. Damour, B. R. Iyer and B. S. Sathyaprakash, "A comparison of search templates for gravitational waves from binary inspiral: 3.5-PN update", Phys. Rev. D 66, 027502 (2002), *ibid* D 66,027502 (2002).

[41] T. Damour, B. R. Iyer, P. Jaranowski and B. S. Sathyaprakash, "Gravitational waves from black hole binary inspiral and merger: The span of third post-Newtonian effective-one-body templates", Phys. Rev. D 67,064028 (2003).

[42] A. Buonanno, Y. Chen and M. Vallisneri, "Detection template families for gravitational waves from the final stages of binary black-holes binaries: Nonspinning case", Phys. Rev. D 67, 024016 (2003), erratum-ibid. D 74, 029903(E) (2006).

[43] L. Blanchet, B. Iyer, C. Will and A. Wiseman, "Gravitational waveforms from inspiralling compact binaries to second-post-Newtonian order", Class. Quantum Grav. 13, 575 (1996).

[44] T. Damour, P. Jaranowski and G. Schafer, "On the determination of the last stable orbit for circular general relativistic binaries at the third post-Newtonian approximation", Phys. Rev. D 62,084011 (2000).

[45] P. Ajith, B. Iyer, C. Robinson and B. Sathyaprakash, "New class of post-Newtonian approximants to the waveform templates of inspiralling compact binaries: Test mass in the Schwarzschild spacetime", Phys. Rev. D **71**, 044029 (2005), erratum, *ibid* 72, 049902 (2005).

[46] A. Gopakumar and B. R. Iyer, "Gravitational waves from inspiralling compact binaries: Angular momentum flux, evolution of the orbital elements, and the waveform to the second post-Newtonian order", Phys. Rev. D 56,7708 (1997).

[47] T. Damour, A. Gopakumar and B. R. Iyer, "Phasing of gravitational waves from inspiralling eccentric binaries", Phys. Rev. D 70,064028 (2004).

[48] L. Kidder, C. Will and A. Wiseman, "Spin effects in the inspiral of coalescing compact binaries", Phys. Rev. D 47, R4183 (1993).

[49] A. Buonanno, Y. Chen and T. Damour, "Transition from inspiral to plunge in precessing binaries of spinning black holes", (2005).

[50] H. Tagoshi and M. Sasaki, "Post-Newtonian expansion of gravitational-waves from a particle in circular orbit around a Schwarzschild black-hole", Prog. Theor. Phys. 92, 745 (1994).

[51] Y. Mino, M. Sasaki, M. Shibata, H. Tagoshi and T. Tanaka, "Black Hole Perturbation", Prog. Theor. Phys. Suppl. 128, 1 (1997).

[52] R. Geroch and G. Horowitz, "Asymptotically simple does not imply asymptotically Minkowskian", Phys. Rev. Lett. 40, 203 (1978).

[53] R. Hansen, "Multipole moments of stationary space-times", J. Math. Phys. 15, 46 (1974).

[54] K. Thorne, "Multipole expansions of gravitational radiation", Rev. Mod. Phys. 52, 299 (1980).

[55] R. Beig and W. Simon, Proc. Roy. Soc. Lond. A 376,333 (1981).

[56] H. Bondi, M. van der Burg and A. Metzner, "Gravitational waves in general relativity **VII.** Waves from axi-symmetric isolated systems", Proc. R. Soc. London, Ser. A 269, 21 (1962).

[57] R. Sachs, "Gravitational Waves in General Relativity. **VI.** Outgoing Radiation Condition", Proc. R. Soc. London, Ser. A **264**, 309+ (1961).

[58] R. Sachs, "Gravitational waves in general relativity. **VIII.** Waves in asymptotically flat space-time", Proc. R. Soc. London, Ser. A 270, 103 (1962).

[59] W. Bonnor and M. Rotenberg, "Transport of momentum by gravitational waves - Linear approximation", Proc. R. Soc. London, Ser. A 265, 109 (1961).

[60] W. Bonnor and M. Rotenberg, "Gravitational waves from isolated sources", Proc. R. Soc. London, Ser. A 289,247 (1966).

[61] L. Blanchet and T. Damour, "Multipolar radiation reaction in general relativity", Phys. Lett. A 104, 82 (1984).

[62] L. Blanchet and T. Damour, "Radiative gravitational fields in general relativity **I.** general structure of the field outside the source", Phil. Trans. Roy. Soc. Lond. **A** 320, 379 (1986).

[63] L. Blanchet and T. Damour, "Tail transported temporal correlations in the dynamics of a gravitating system", Phys. Rev. D 37, 1410 (1988).

[64] L. Blanchet, "Radiative gravitational fields in general-relativity. II. Asymptotic-behaviour at future null infinity", Proc. R. Soc. London, Ser. A 409,383 (1987).

[65] T. Damour, "Gravitational radiation and the motion of compact bodies", in ***Gravitational Radiation,*** edited by N. Deruelle and T. Piran, pages 59–144 (North-Holland Company, Amsterdam, 1983).

[66] A. Einstein, "Über Gravitationswellen", Sitzungsber. K. Preuss. Akad. Wiss. 1918, 154 (1918).

[67] L. Landau and E. Lifshitz, ***The classical theory of fields*** (Pergamon, Oxford, 1971).

[68] D. Landau and E. A. Lifshitz, editors, ***Teoriya Polya*** (Nauka, Moscow, 1941).

[69] V. A. Fock, editor, ***Teoriya prostranstva vremeni i tyagoteniya*** (Fizmatgiz, Moscow, 1955).

[70] R. Epstein and R. Wagoner, "Post-Newtonian generation of gravitational-waves", Astrophys. J. 197,717 (1975).

[71] K. S. Thorne, "The Generation of Gravitational Waves: A Review of Computational Techniques", in ***NATO ASZB Proc. 27: Topics in Theoretical and Experimental Gravitation Physics,*** edited by ***V.*** de Sabbata and J. Weber, page 1 (1977).

[72] J. L. Anderson, "New Derivations of the Quadrupole Formulas and Balance Equations for Gravitationally Bound Systems", Phys. Rev. Lett. 45, 1745 (1980).

[73] M. Walker and C. M. Will, "Gravitational radiation quadrupole formula is valid for gravitationally interacting systems", Phys. Rev. Lett. 45, 1741 (1980).

[74] T. Damour, ***The problem of motion in Newtonian and Einsteinian gravity,*** pages 128–198 (Cambridge University Press, 1987).

[75] L. Blanchet and T. Damour, "Post-Newtonian generation of gravitational waves", .

[76] L. Blanchet and T. Damour, "Hereditary effects in gravitational radiation", Phys. Rev. D 46,4304 (1992).

[77] L. Blanchet, T. Damour and B. R. Iyer, "Gravitational waves from inspiralling compact binaries: Energy loss and wave form to second post-Newtonian order", Phys. Rev. D 51,5360 (1995).

[78] W. Bonnor, "Spherical gravitational waves", Philos. Trans. R. Soc. London, Ser. A 251,233 (1959).

[79] C. Will and A. Wiseman, "Gravitational radiation from compact binary systems: Gravitational waveforms and energy loss to second post-Newtonian order", Phys. Rev. D 54,4813 (1996).

[80] T. Futarnase and B. F. Schutz, "Gravitational radiation and the validity of the far-zone quadrupole formula in the Newtonian limit of general relativity", Phys. Rev. D 32, 2557 (1985).

[81] T. Futamase, "Point-particle limit and the far-zone quadrupole formula in general relativity", Phys. Rev. D 32,2566 (1985).

[82] Y. Itoh and T. Futamase, "New derivation of a third post-Newtonian equation of motion for relativistic compact binaries without ambiguity", Phys. Rev. D 68, 121501(R) (2003).

[83] T. Damour, "Gravetional radiation reaction in the binary pulser and the quadrupole formula controversy", Phys. Rev. Lett. 51, 1019 (1983).

[84] L. Blanchet, G. Faye and B. Ponsot, "Gravitational field and equations of motion of compact binaries to 5/2 post-Newtonian order", Phys. Rev. D 58, 124002 (1998).

[85] L. Blanchet and G. Faye, "Equations of motion of point-particle binaries at the third post-Newtonian order", Phys. Lett. A **271**, 58 (2000).

[86] L. Blanchet and G. Faye, "General relativistic dynamics of compact binaries at the third post-Newtonian order", Phys. Rev. D 63,062005 (2001).

[87] T. Damour, P. Jaranowski and G. Schafer, "Dimensional regularization of the gravitational interaction of point masses", Phys. Lett. B 513, 147 (2001).

[88] T. Damour, P. Jaranowski and G. Schafer, "Equivalence between the ADM-Hamiltonian and the harmonic-coordinates approaches to the third post-Newtonian dynamics of compact binaries", Phys. Rev. D 63, 044021 (2001), erratum, ibid, 66, 029901(E) (2002).

[89] T. Damour, P. Jaranowski and G. Schafer, "Poincaré invariance in the ADM Hamiltonian approach to the general relativistic two-body problem", Phys. Rev. D 62, 021501(R) (2000), erratum, ibid, **63**, 029903(E) (2000).

[90] P. Jaranowski and G. Schafer, "The binary black-hole dynamics at the third post-Newtonian order in the orbital motion", Ann. Phys. (Berlin) 9,378 (2000).

[91] P. Jaranowski and G. Schafer, "Radiative 3.5 post-Newtonian ADM Hamiltonian for many body point - mass systems", Phys. Rev. D 55,4712 (1997).

[92] P. Jaranowski and G. Schafer, "Third post-Newtonian higher order ADM Hamilton dynamics for two-body point-mass systems", Phys. Rev. D 57,7274 (1998).

[93] P. Jaranowski and G. Schafer, "The binary black-hole problem at the third post-Newtonian approximation in the orbital motion: Static part", Phys. Rev. D **60,** 124003 (1999).

[94] P. Jaranowski and G. Schafer, "Binary black-hole problem at the third post-Newtonian approximation in the orbital motion: Static part", Phys. Rev. D 60, 124003 (1999).

[95] L. Blanchet, B. R. Iyer and B. Joguet, "Gravitational waves from inspiralling compact binaries: Energy flux to third post-Newtonian order", Phys. Rev. D 65,064005 (2002), Erratum Phys. Rev. D71, 129903(E) (2005).

[96] L. Blanchet and B. R. Iyer, "Hadamard regularization of the third post-Newtonian gravitational wave generation of two point masses", Phys. Rev. D 71,024004 (2005).

[97] L. Blanchet, "Second post-Newtonian generation of gravitational radiation", Phys. Rev. D 51,2559 (1995).

[98] L. Blanchet, "On the multipole expansion of the gravitational field, Class. Quantum Grav. 15, 1971 (1998).

[99] T. Damour and B. R. Iyer, "Post-Newtonian generation of gravitational waves. 2. The Spin moments", Annales Inst. H. Poincaré, Phys. Théor. 54, 115 (1991).

[100] T. Damour and B. R. Iyer, "Multipole analysis for electromagnetism and linearized gravity with irreducible cartesian tensors", Phys. Rev. D 43, 3259 (1991).

[101] G. 't Hooft and M. Veltman, "Regularization and renormalization of gauge fields", Nucl. Phys. B 44, 189 (1972).

[102] L. Blanchet, T. Damour and G. Esposito-Farèse, "Dimensional regularization of the third post-Newtonian dynamics of point particles in harmonic coordinates", Phys. Rev. D 69, 124007 (2004).

[103] M. Pati and C. Will, "Post-Newtonian gravitational radiation and equations of motion via direct integration of the relaxed Einstein equations: Foundations", Phys. Rev. D **62,** 124015 (2000).

[104] M. Pati and C. Will, "Post-Newtonian gravitational radiation and equations of motion via direct integration of the relaxed Einstein equations. II. Two-body equations of motion to second post-Newtonian order, and radiation-reaction to 3.5 post-Newtonian order", Phys. Rev. D 65, 104008 (2002).

[105] L. Blanchet, G. Faye and S. Nissanke, "Post-Newtonian expansion including gravitational radiation reaction", (2004), work in preparation.

[106] L. Blanchet, G. Faye and S. Nissanke, "Structure of the post-Newtonian expansion in general relativity", Phys. Rev. D 72,044024 (2005).

[107] S. Nissanke and L. Blanchet, "Gravitational radiation reaction in the equations of motion of compact binaries to 3.5 post-Newtonian order", Class. Quantum Grav. 22, 1007 (2005).

[108] L. Blanchet, G. Faye, B. R. Iyer and B. Joguet, "Gravitational-wave inspiral of compact binary systems to 7/2 post-Newtonian order", Phys. Rev. D **65**, 061501(R) (2002), Erratum Phys. Rev. D71, 129902(E) (2005).

[109] L. Blanchet, T. Damour, G. Esposito-Farèse and B. R. Iyer, "Gravitational radiation from inspiralling compact binaries completed at the third post-Newtonian order", Phys. Rev. Lett. 93,091101 (2004).

[110] K. G. Arun, L. Blanchet, B. R. Iyer and M. S. Qusailah, "The 2.5PN gravitational wave polarisations from inspiralling compact binaries in circular orbits", Class. Quantum Grav. 21,3771 (2004), erratum-ibid. **22**, 3115 (2005).

[111] P. C. Peters and J. Mathews, "Gravitational Radiation from Point Masses in a Keplerian Orbit", Physical Review 131,435 (1963).

[112] P. Peters, "Gravitational Radiation and the Motion of Two Point Masses", Phys. Rev. 136, B1224 (1964).

[113] C. W. Lincoln and C. M. Will, "Coalescing binary systems of compact objects to $(post)^{5/2}$-Newtonian order: Late-time evolution and gravitational-radiation emission", Phys. Rev. D 42, 1123 (1990).

[114] C. Moreno-Garrido, E. Mediavilla and J. Buitrago, "Gravitational radiation from point masses in elliptical orbits: spectral analysis and orbital parameters", Mon. Not. R. Astron. Soc. 274, 115 (1995).

[115] A. Gopakumar and B. R. Iyer, "Second post-Newtonian gravitational wave polarizations for compact binaries in elliptical orbits", Phys. Rev. D 65,084011 (2002).

[116] K. Glampedakis, S. A. Hughes and D. Kennefick, "Approximating the inspiral of test bodies into Kerr black holes", Phys. Rev. D 66,064005 (2002).

[117] L. Wen, "On the Eccentricity Distribution of Coalescing Black Hole Binaries Driven by the Kozai Mechanism in Globular Clusters", Astrophys. J 598,419 (2003).

[118] Y. Kozai, "Secular perturbations of asteroids with high inclination and eccentricity", Astron. Journa 67, 591 (1962).

[119] T. A. Moore and R. W. Hellings, "The Angular Resolution of Space-Based Gravitational Wave Detectors", Phys. Rev. D 65,062001 (2002).

[120] L. Wen, "On the Eccentricity Distribution of Coalescing Black Hole Binaries Driven by the Kozai Mechanism in Globular Clusters", Astrophys. J 598,419 (2003).

[121] M. J. Benacquista, "Relativistic Binaries in Globular Clusters", Living Rev. Relativity 5, 2 (2002), http://www.livingreviews.org/lrr-2002-2.

[122] K. Giiltekin, M. C. Miller and H. D. P, "Growth of Intermediate-Mass Black Holes in Globular Clusters", Astrophys. J 616, 221 (2004).

[123] 0 . Blaes, M. H. Lee and A. Socrates, "The Kozai Mechanism and the Evolution of Binary Supermassive Black Holes", The Astrophys. J 578,775 (2002).

[124] J. Bekenstein, "Gravitational Radiation Recoil and Runaway Black Holes", Astrophys. J. 183,657 (1973).

[125] E. R. Harrison and E. Tademaru, "Acceleration of pulsars by asymmetric radiation", Astrophys. J 201,447 (1975).

[126] D. Lai, D. F. Chernoff and J. M. Cordes, "Pulsar Jets: Implications for Neutron Star Kicks and Initial Spins", Astrophys. J 549, 1111 (2001).

[127] M. J. Fitchett, "The influence of gravitational wave momentum losses on the centre of mass motion of a Newtonian binary system", mnras 203, 1049 (1983).

[128] I. H. Redmount and M. J. Rees, "Gravitational-radiation rocket effects and galactic structure .", Comments on Astrophysics 14, 165 (1989).

[129] D. Merritt, M. Milosavljevic, M. Favata, S. A. Hughes and D. E. Holz, "Consequences of gravitational radiation recoil", The Astrophys. J 607, L9 (2004).

[130] J. M. Weisberg and J. H. Taylor, "The Relativistic Binary Pulsar B1913+16: Thirty Years of Observations and Analysis", in ***ASP Conf. Ser. 328: Binary Radio Pulsars,*** edited by F. A. Rasio and I. H. Stairs, pages 25–+ (2005).

[131] A. G. Lyne, M. Burgay, M. Kramer, A. Possenti, R. N. Manchester, F. Camilo, M. A. McLaughlin, D. R. Lorimer, N. D'Amico, B. C. Joshi, J. Reynolds and P. C. C. Freire, "A Double-Pulsar System: A Rare Laboratory for Relativistic Gravity and Plasma Physics", Science 303, 1153 (2004).

[132] M. Kramer, A. G. Lyne, M. Burgay, A. Possenti, R. N. Manchester, F. Camilo, M. A. McLaughlin, D. R. Lorimer, N. D'Amico, B. C. Joshi, J. Reynolds and P. C. C. Freire, "The Double Pulsar – A New Testbed for Relativistic Gravity", in ***ASP Conf. Ser. 328: Binary Radio Pulsars,*** edited by F. A. Rasio and I. H. Stairs, pages 59–+ (2005).

[133] I. H. Stairs, "Testing General Relativity with Pulsar Timing", Living Reviews in Relativity **6**, 5 (2003).

[134] B. C. Barish and R. Weiss, "LIGO and the detection of gravitational waves.", Physics Today **52**, 44 (1999).

[135] C. Will, "Generation of Post-Newtonian Gravitational Radiation via Direct Integration of the Relaxed Einstein Equations", Prog. Theor. Phys. Suppl. 136, 158 (1999).

[136] C. M. Will, "Bounding the mass of the graviton using gravitational-wave observations of inspiralling compact binaries", Phys. Rev. D 57,2061 (1998).

[137] C. Cutler, T. Apostolatos, L. Bildsten, L. Finn, E. Flanagan, D. Kennefick, D. Marković, A. Ori, E. Poisson, G. Sussman and K. Thorne, "The last three minutes: Issues in gravitational wave measurements of coalescing compact binaries", Phys. Rev. Lett. 70, 2984 (1993).

[138] P. Peters and J. Mathews, "Gravitational Radiation from Point Masses in a Keplerian Orbit", Phys. Rev. 131,435 (1963).

[139] M. Burgay, N. D'Amico, A. Possenti, R. Manchester, A. Lyne, B. C. Joshi, M. A. McLaughlin, M. Kramer, J. M. Sarkissian, C. F, V. Kalogera, C. Kim and D. R. Lorimer, "An increased estimate of the merger rate of double neutron stars from observations of a highly relativistic system", Nature 426, 531 (2003).

[140] L. A. Wainstein and V. D. Zubakov, ***Extraction of Signals from Noise*** (Prentice-Hall, Englewood Cliffs, 1962).

[141] K. S. Thorne and V. B. Braginskii, "Gravitational-wave bursts from the nuclei of distant galaxies and quasars - Proposal for detection using Doppler tracking of interplanetary spacecraft", Astrophys. J 204, L1 (1976).

[142] R. Wagoner and C. Will, "Post-Newtonian gravitational radiation from orbiting point masses", Astrophys. J. 210,764 (1976).

[143] L. Blanchet and G. Schafer, "Higher order gravitational radiation losses in binary systems", Mon. Not. Roy. Astron. Soc. 239, 845 (1989).

[144] W. Junker and G. Schaefer, "Binary systems - Higher order gravitational radiation damping and wave emission", Monthly Notices of the Royal Astronomical Society 254,146 (1992).

[145] L. Blanchet and G. Schafer, "Gravitational wave tails and binary star systems", Class. Quantum Grav. 10,2699 (1993).

[146] R. Rieth and G. Schafer, "Spin and tail effects in the gravitational-wave emission of compact binaries", Class. Quantum Grav. 14,2357 (1997).

[147] T. Damour and N. Deruelle, "General relativistic celestial mechanics of binary systems I. The post-Newtonian motion", Annales Inst. H. Poincaré Phys. Théor. 43, 107 (1985).

[148] T. Damour and G. Schafer, "Higher order relativistic periastron advances binary pulsars", Nuovo Cim. **B101**, 127 (1988).

[149] G. Schafer and N. Wex, "Second post-Newtonian motion of compact binaries", Phys. Lett. A 174, 196 (1993), Erratum, *ibid*, **177**, 461(E) (1993).

[150] N. Wex, "The second post-Newtonian motion of compact binary-star systems with spin", Classical Quant. Grav. 12,983 (1995).

[151] C. Will and A. Wiseman, "Gravitational radiation from compact binary systems: Gravitational waveforms and energy loss to second post-Newtonian order", Phys. Rev. D **54**, 4813 (1996).

[152] L. Blanchet and G. Faye, "Hadamard regularization", J. Math. Phys. 41,7675 (2000).

[153] L. Blanchet, T. Damour and B. R. Iyer, "Surface-integral expressions for the multipole moments of post-Newtonian sources and the boosted Schwarzschild solution", Class. Quantum Grav. 22, 155 (2005).

[154] L. Blanchet, T. Damour, G. Esposito-Farèse and B. R. Iyer, "Dimensional regularization of the third post-Newtonian gravitational wave generation of two point masses", Phys. Rev. D 71, 124004 (2005).

[155] R. Mernmesheimer, A. Gopakumar and G. Schafer, "Third post-Newtonian accurate generalized quasi-Keplerian parametrization for compact binaries in eccentric orbits", Phys. Rev. D 70, 104011 (2004).

[156] L. Blanchet, "Energy losses by gravitational radiation in inspiralling compact binaries to five halves post-Newtonian order", Phys. Rev. D 54, 1417 (1996), Erratum Phys. Rev. D71, 129904(E) (2005).

[157] L. Blanchet, "Quadrupole-quadrupole gravitational waves", Class. Quantum Grav. 15, 89 (1998).

[158] L. Blanchet, "Gravitational-wave tails of tails", Class. Quantum Grav. 15, 113 (1998).

[159] L. Blanchet and B. R. Iyer, "Third post-Newtonian dynamics of compact binaries: Equations of motion in the center-of-mass frame", Class. Quantum Grav. 20, 755 (2003).

[160] V. de Andrade, L. Blanchet and G. Faye, "Third post-Newtonian dynamics of compact binaries: Noetherian conserved quantities and equivalence between the harmonic-coordinate and ADM-Hamiltonian formalisms", Class. Quantum Grav. 18, 753 (2001).

[161] T. Mora and C. M. Will, "A post-Newtonian diagnostic of quasi-equilibrium binary configurations of compact objects", Phys. Rev. D 69, 104021 (2004).

[162] M. Sasaki and H. Tagoshi, "Analytic Black Hole Perturbation Approach to Gravitational Radiation", Living Rev. Relativity 6, 6 (2003).

[163] C. Koenigsdoerffer and A. Gopakumar, "Phasing of gravitational waves from inspiralling eccentric binaries at the third-and-a-half post-Newtonian order", (2006).

[164] D. Christodoulou, "Nonlinear nature of gravitation and gravitational-wave experiments", Phys. Rev. Lett. 67, 1486 (1991).

[165] A. Wiseman and C. Will, "Christodoulou's nonlinear gravitational-wave memory: Evaluation in the quadrupole approximation", Phys. Rev. D 44, R2945 (1991).

[166] K. Thorne, "Gravitational-wave bursts with memory: The Christodoulou effect", Phys. Rev. D 45, 520 (1992).

[167] L. Blanchet and B. S. Sathyaprakash, "Signal analysis of gravitational wave tails", Class. Quantum Grav. 11,2807 (1994).

[168] L. Blanchet and B. S. Sathyaprakash, "Detecting the tail effect in gravitational wave experiments", Phys. Rev. Lett. 74, 1067 (1995).

[169] K. G. Arun, B. R. Iyer, M. S. S. Qusailah and Sathyaprakash, "Testing post-Newtonian theory with gravitational wave observations", Class. Quantum Grav. 23, L37 (2006).

[170] K. G. Arun, B. R. Iyer, M. S. S. Qusailah and Sathyaprakash, "Testing post-Newtonian theory with gravitational wave observations", (2006), (submitted).

[171] T. Damour and N. Deruelle, "General relativistic celestial mechanics of binary systems II. The post-Newtonian timing formula", Annales Inst. H. Poincaré Phys. Théor. 44,263 (1986).

[172] A. Peres, "Classical Radiation Recoil", Physical Review 128,2471 (1962).

[173] J. D. Bekenstein, "Gravitational-Radiation Recoil and Runaway Black Holes", Astrophys.J. 183,657 (1973).

[174] C. T. Cunningharn, R. H. Price and V. Moncrief, "Radiation from collapsing relativistic stars. I - Linearized odd-parity radiation", Astrophys. J. 224, 643 (1978).

[175] C. T. Cunningharn, R. H. Price and V. Moncrief, "Radiation from collapsing relativistic stars. II - Linearized even-parity radiation", Astrophys. J. 230, 870 (1979).

[176] V. Moncrief, "Radiation from collapsing relativistic stars. IV - Black hole recoil", Astrophys. J. 238,333 (1980).

[177] K. Oohara and T. Nakamura, "Energy, Momentum and Angular Momentum of Gravitational Waves Induced by a Particle Plunging into a Schwarzschild Black Hole", Progress of Theoretical Physics 70,757 (1983).

[178] M. J. Fitchett and S. Detweiler, "Linear momentum and gravitational waves - Circular orbits around a Schwarzschild black hole", mnras 211, 933 (1984).

[179] A. Papapetrou, Ann. Inst. Henri Poincaré XIV, 79 (1962).

[180] L. Blanchet, "Gravitational radiation reaction and balance equations to post-Newtonian order", Phys. Rev. D 55, 714 (1997).

[181] M. Favata, S. A. Hughes and D. E. Holz, "How black holes get their kicks: Gravitational radiation recoil revisited", Astrophys. J. 607, L5 (2004).

[182] A. G. Wiseman, "Coalescing binary systems of compact objects to (post) $^{5/2}$-Newtonian order. II. Higher-order wave forms and radiation recoil", Phys. Rev. D 46, 1517 (1992).

[183] B. R. Iyer and C. M. Will, "Post-Newtonian gravitational radiation reaction for two-body systems: Nonspinning bodies", Phys. Rev. D 52,6882 (1995).

[184] C. Konigsdorffer, G. Faye and G. Schafer, Phys. Rev. D **68**, 044004 (2003).

[185] T. Damour, "Coalescence of two spinning black holes: An effective one-body approach", Phys. Rev. D 64, 124013 (2001).

[186] T. Nakamura and M. P. Haugan, "Gravitational radiation from particles falling along the symmetry axis into a Kerr black hole - The momentum radiated, Astrophys.J. 269,292 (1983).

[187] M. Campanelli, "Understanding the fate of merging supermassive black holes", Classical Quant. Grav. 22, S387 (2005).

[188] O. K. . K. Y. Nakamura, T., Prog. Theor. Phys. Supp. 90, 1 (1987).

[189] T. Damour and A. Gopakumar, "Gravitational Recoil during Binary Black Hole Coalescence using the Effective One Body Approach", (2006).

[190] J. G. Baker, J. Centrella, D.-I. Choi, M. Koppitz, J. R. van Meter and M. C. Miller, "Getting a kick out of numerical relativity", (2006).

[191] L. E. Kidder, "Coalescing binary systems of compact objects to (post)$^{5/2}$-Newtonian order. V. Spin effects", Phys. Rev. D 52, 821 (1995).

[192] C. M. Will, "The Confrontation between General Relativity and Experiment", Living Rev. Relativity 9, 3 (2006).

[193] T. Damour and J. Taylor, "Strong-field tests of relativistic gravity and binary pulsars", Phys. Rev. D 45, 1840 (1992).

[194] W. J. M and T. J. H, "The Relativistic Binary Pulsar B1913+16", (2003).

[195] C. M. Will, "Bounding the mass of the graviton using gravitional-wave observations of inspiralling compact binaries", Phys. Rev D 57,2061 (1998).

[196] E. Berti, A. Buonanno and C. M. Will, "Estimating spinning binary parameters and testing alternative theories of gravity with LISA", Phys. Rev. D 71,084025 (2005).

[197] C. M. Will, "Testing Scalar-Tensor Gravity with Gravitational-Wave Observations of Inspiralling Compact Binaries", Phys. Rev. D 50,6058 (1994).

[198] P. D. Scharre and C. M. Will, "Testing Scalar-Tensor Gravity Using Space Gravitational-Wave Interferometers", Phys. Rev. D 65, 042002 (2002).

[199] T. Damour and G. Esposito-Farbse, "Tensor-scalar gravity and binary-pulsar experiments", Phys. Rev. D 54, 1474 (1996).

[200] L. Blanchet, T. Damour, B. R. Iyer, C. M. Will and A. G. Wiseman, "Gravitational radiation damping of compact binary systems to second post-Newtonian order", Phys. Rev. Lett. 74,3515 (1995).

[201] B. S. Sathyaprakash and S. V. Dhurandhar, "Choice of filters for the detection of gravitational waves from coalescing binaries", Phys. Rev. D 44, 3819 (1991).

[202] C. Cutler and K. S. Thorne, "An Overview of Gravitational-Wave Sources", (2002).

[203] M. Punturo (Private communication).

[204] C. Van Den Broeck and A. Sengupta, "Phenomenology of amplitude-corrected post-Newtonian gravitational waveforms for compact binary inspiral. I. Signal-to-noise ratios", (2006).

[205] W. H. Press, S. A. Teukolsky, W. T. Vetterling and B. P. Flannery, ***Numerical Recipes in C++: The Art of Scientific Computing*** (Cambridge University Press, 2002), 2nd edition.

[206] C. Cutler, "Angular resolution of the LISA gravitational wave detector", Phys. Rev. D 57,7089 (1998).

[207] L. Barack and C. Cutler, "Confusion noise from LISA capture sources", Phys. Rev. D 70, 122002 (2004).

[208] L. Barack and C. Cutler, "LISA Capture Sources: Approximate Waveforms, Signal-to-Noise Ratios, and Parameter Estimation Accuracy", Phy. Rev. D **69,** 082005 (2004).

[209] K. G. Arun, "Parameter estimation of coalescing supermassive black hole binaries with LISA", Phys. Rev. **D74**, 024025 (2006).

[210] T. Damour and G. Esposito-Farèse, "Gravitational-wave versus binary-pulsar tests of strong-field gravity", Phys. Rev. D 58,042001 (1998).

[211] T. Damour and J. Taylor, "Strong-field tests of relativistic gravity and binary pulsars", Phys. Rev. D 45, 1840 (1992).

[212] J. Taylor and J. Weisberg, "A New Test of General Relativity: Gravitational Radiation and the Binary Pulsar PSR 1913+16", Astrophys. J. 253,908 (1982).

[213] C. Will, "Gravitational Waves from Inspiralling Compact Binaries: A Post-Newtonian Approach", in Relativistic Cosmology, edited by M. Sasaki, volume 8 of Nishinomiya-Yukawa Symposium Series, pages 83–98 (Universal Academy Press, Tokyo, 1994).

[214] K. G. Arun, B. R. Iyer, B. S. Sathyaprakash and P. A. Sundararajan, "Parameter estimation of inspiralling compact binaries using 3.5 post-Newtonian gravitational wave phasing: The non-spinning case", Phys. Rev. D **71,** 084008 (2005), erratum-ibid. D 72,069903 (2005).

[215] http://www.astro.cf.ac.uk/geo/ego/.

[216] T. Damour and G. Esposito-Farèse, "Tensor multiscalar theories of gravitation", Class. Quantum Grav. 9,2093 (1992).

[217] L. Blanchet, A. Buonanno and G. Faye, "Higher-order spin effects in the dynamics of compact binaries II. Radiation field, (2006), article submitted.

[218] G. Faye, L. Blanchet and A. Buonanno, "Higher-order spin effects in the dynamics of compact binaries I. Equations of motion", (2006), article submitted.

[219] A. Krolàk, K. Kokkotas and G. Schafer, "Estimation of the post-Newtonian parameters in the gravitational-wave emission of a coalescing binary", Phys. Rev. D 52,2089 (1995).

[220] M. Luna and A. M. Sintes, "Parameter estimation of compact binaries using the inspiral and ringdown waveforms", Class. Quantum Grav 23,3763 (2006).

[221] C. Van Den Broeck, "Binary black hole detection rates in inspiral gravitational wave searches", (2006).

[222] R. W. Hellings and T. A. Moore, "The information content of gravitational wave harmonics in compact binary inspiral", Class. Quant. Grav. 20, S181 (2002).

[223] M. Tinto and S. Dhurandhar, "Time-Delay Interferometry", Living Rev. Relativity **8,** 4 (2005).